5. Application notes

Introduction

During the development, Alecsis was constantly verified on a large number of different examples. Also, it was used in some real projects, where different electronic circuits have been designed. We will give here some of the typical simulation examples where Alecsis is presented as a circuit and system (mixed-domain) simulator, used in different analogue, discrete-event and mixed-signal applications.

The first example is an analog multiplier, where Alecsis is used as a circuit simulator, i.e. equivalently as SPICE. SPICE compatibility is enabled through the usage of similar syntax rules and same syntax of model card. In the next two examples of SC filter and switching flyback converter, Alecsis is used also as a circuit simulator. Nevertheless, an ideal switch model that is a peculiar feature of Alecsis is used there. Such simulations cannot be so easily performed in other circuit simulators.

After that, five examples are given that depict analogue modeling features of AleC++. Firstly, a representation of MOS transistor modeling using neural network is given. After that, example of fuzzy-logic control system is presented.

Variables used there for modeling are not only of electronic, but also of very abstract nature. An example of control system modeling using transfer functions is given after that. Later on, example of electromechanical system modeling is presented through a nonlinear electromagnetic circuit. As a last example of analogue modeling features of Alecsis, a pressure sensing system is used. In this electromechanical simulation, space-continuous models, i.e. partial differential equations, are described in AleC++.

Ninth and tenth example in this section are of discrete-event simulation. In the systolic array circuit, AleC++ is used for modeling of logic circuits. After that, in LAN network simulation, models of more abstract discrete-event systems are described.

Three examples of mixed-mode and mixed-signal simulation are also presented. For A/D converter simulation, analogue and logic circuitry are coupled. In the next example, sigma-delta modulator is simulated, which is considered to be one of the benchmark tests for mixed-mode simulation. The last example of this group is pressure sensor simulation, with analogue readout circuitry and analog signal conversion into a discrete value. Therefore, in this example mixed-domain, mixed-signal and mixed-mode simulation is performed.

In discrete-event system modeling, Alecsis is able to support not also AleC++, but also VHDL. The last example in this chapter gives such AleC++ / VHDL co-simulation.

In the examples throughout this chapter some characteristic parts of model code are given. They are used just to illustrate usage of the modeling language AleC++. For learning the syntax of the language, Alecsis User's Manual is available.

5.1. Analogue multiplier simulation

The common way of analog systems modeling is structural description that stands for coupling of components with links and definition of components' parameters. As an example of pure structural description, the analog multiplier shown in Fig. 5.1 will be considered. It consists of 19 MOS transistors, and has the following functional blocks: pre-distortion circuit, voltage controlled current source, and two differential stages. Multiplier output is between nodes 18 and 19.

Multiplier is described structurally in a way that circuit elements are first declared:

```
resistor r1,r2;
```

meaning that components `r1` and `r2` are resistors. It is also possible to use implicit declaration:

```
implicit { resistor r; capacitor c; }
```

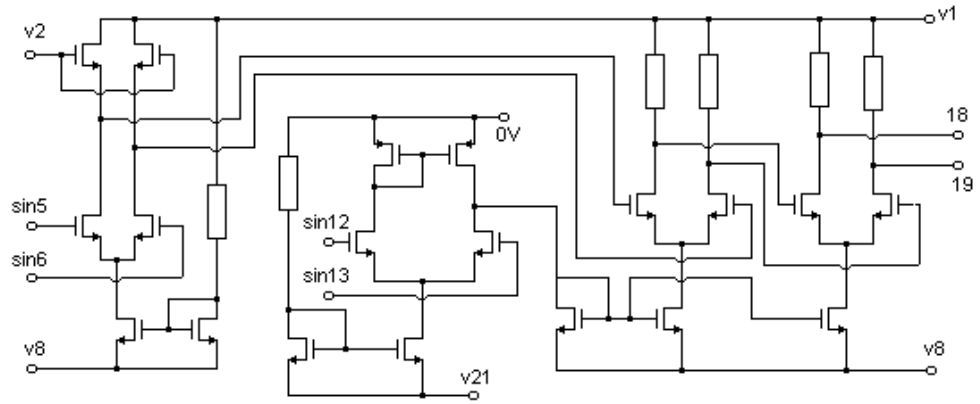

Fig. 5.1: Analog multiplier with MOS transistors

which means that all elements beginning with `r` are resistors, and all ones beginning with `c` are capacitors.

After declaring the components to be used, structural description of the multiplier is similar to SPICE circuit description. Nodes where the component is plugged are given in parenthesis, and parameters (including the name of the model card) are given afterwards. A part of the code describing the multiplier is given that shows the instantiation of an MOS transistor.

```
mp2 (11,10,0,0) { model=PC_PM1; w=1.7u; l=1.2u;
                  ad=150p; as=100p; pd=10p; ps=10p; }
```

Of course, the model card `PC_PM1` must be defined earlier in the simulation library. It has the same syntax as SPICE MOS model, so it will not be described in details here.

To demonstrate the simulation of the multiplier depicted in Fig. 5.1, two sine wave signals with different frequencies are brought to its inputs. Multiplier output is an amplitude-modulated signal. The simulation results are given in Fig. 5.2.

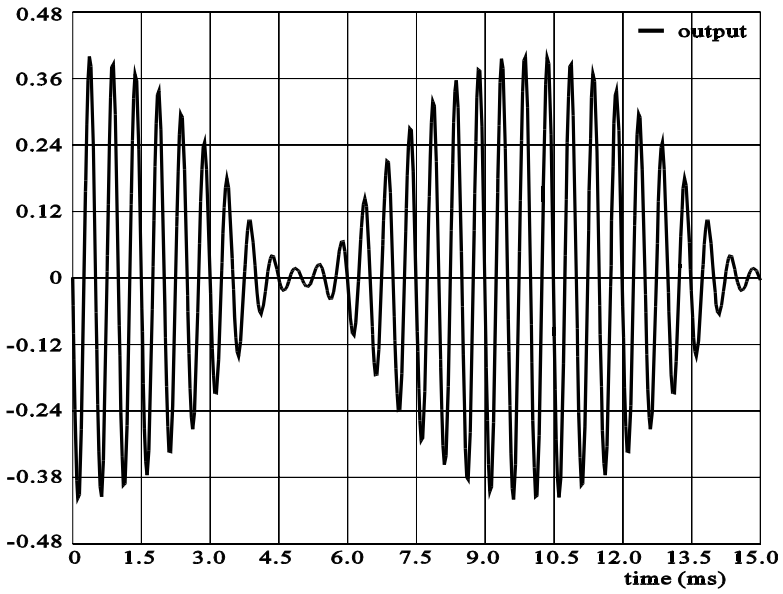

Fig. 5.2: Results of analog multiplier simulation

5.2. SC filter

This example also employs only structural description. The circuit shown in Fig. 5.3 contains switches, therefore the ideal switch, an Alecsis built-in component, is used. It should be noted that a truly ideal switch is used, with resistance zero for closed switch and infinite resistance for open switch [`Mr~a93`]

The parameters `val_on` and `val_off` determine voltages that turn switch on and off, respectively. There is another parameter `hyst` that defines switch with hysteresis if set on 1. The switch description requires four nodes: the first two are topological information of switch position in the circuit, and last two are controlling nodes. The double switch from Fig. 5.3 is described as a module named `Double_Switch`. It consists of two switches that charge and discharge capacitors making them behave as they were resistors.

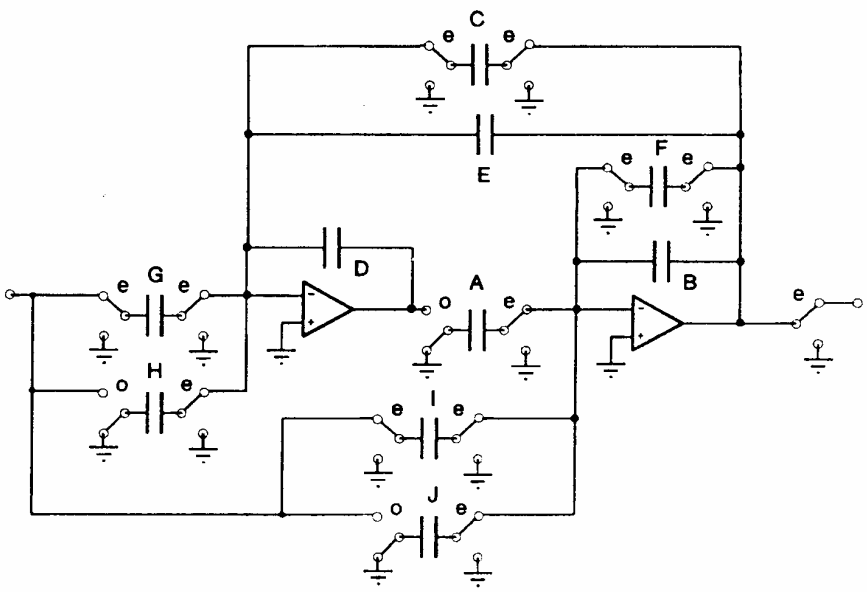

Fig. 5.3: SC filter circuit.

```
module Double_Switch (even,odd,common,commutation) {
       // Declaration section
```

```
            switch se,so;
          // Structural section
            se (common,even,commutation,0) val_on=val_off=0;
            so (common,odd,0,commutation) val_on=val_off=0;
}
```

The SC filter circuit is excited through a sample and hold circuit, shown in Fig 5.4.

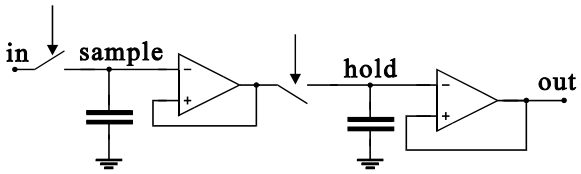

Fig. 5.4: Sample and hold circuit

The sample/hold circuit is also described as a separate module `SH_circuit`, with three interface nodes.

```
module SH_circuit (node input, output, commutation) {
  switch se,so;
  capacitor c1,c2;
  opamp opamp1,opamp2;

  se (input,sample,commutation,0) {val_on=val_off=0;}
  c1 (sample,0) 1pF;
  opamp1 (internal,sample,internal);
  so (internal,hold,0,commutation) {val_on=val_off=0;}
  c2 (hold,0) 1pF;
  opamp2 (output,hold,output) ;
}
```

Switches are controlled by the voltage at the node called `commutation`. Its value, depending on weather it is greater or less than zero, determines state of the switches. Operational amplifiers are modeled as ideal (single voltage controlled source).

For the simulation, sine wave of frequency 128kHz is used to control the switches. In Fig. 5.5 simulation results are shown: excitation and response of the SC filter circuit.

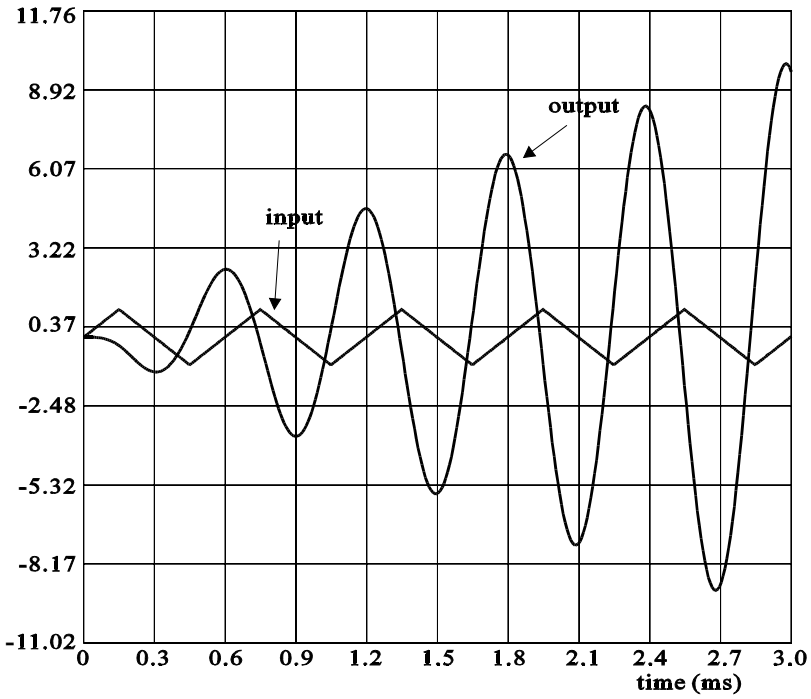

Fig. 5.5: Simulation results for SC circuit excited by triangular input signal.

5.3. Switching voltage regulators

The ideal switch model is suited for all types of circuits. A particularly important class of switched circuits is that of switching voltage regulators. One of the main problems in simulation of such class of circuits is occurrence of inconsistent initial conditions. These conditions occur after switching, when instantaneous change of the capacitor voltage or inductor currents can happen. In such cases, current through capacitor and voltage over inductor have infinite values, but such impulses have infinitely short duration (Dirac impulses). Such problems are usually solved by the application of special algorithms for switched networks [Opal90].

With our model, we have modeled the transition of the switch state, i.e. the switching is not represented just as a replacement of one network topology by another. With our nonlinear model, the switch transition is performed through number of iterations, where, in every iteration, both Kirchhoff laws are satisfied [`Mr~a99`]. Networks with inconsistent initial conditions are solved using standard circuit simulation algorithms. This enables changes in the level of abstraction used in modeling, without change of the simulation environment.

As identified in [Bedr92, Vlac95], the problem of inconsistent initial conditions is not only to conserve the charge and the flux. It is very important to take into account Dirac impulses that can occur in the moment of switching, especially if the network contains internally controlled switches. A Dirac impulse can itself change the states of some switches in the network, thus changing the network topology once more in the same time instant.

The problem will be depicted by the ideal flyback switching converter, given in Fig. 5.6(a). The switch *s* represents the transistor that is externally controlled. The diode *D* is also modeled as ideal switch, but internally controlled. One can model this diode using a control variable *p* [Bedr92]:

$$D:\begin{cases} ON & if\ p>0 \\ OFF & if\ p<0 \end{cases}, \qquad p=\begin{cases} i & if\ D\ \ is\ \ closed \\ v_j - v_k & if\ D\ \ is\ \ open \end{cases}. \qquad (5.1)$$

Therefore, the state of the switch *D* is controlled by the variables in the circuit itself. Let us start the analysis with switch *s* closed and switch *D* open. The equivalent circuit is shown in Fig. 5.6(b). Inductor current i_L is linearly increasing. When *s* is externally opened, the inductor current has no closed loop. Therefore, i_L must drop instantaneously to zero. Because of that, a Dirac impulse of voltage appears at the inductor. This Dirac impulse changes the switch control variable *p* to a positive value (eqn. 5.1.), and D becomes closed. Since Dirac impulse has zero

duration, *D* is closed in the same time instant when *s* is opened. When this happens, the current of the inductor has a closed loop to flow (Fig. 5.6(c)), and there is no discontinuity in the inductor current. Therefore, the

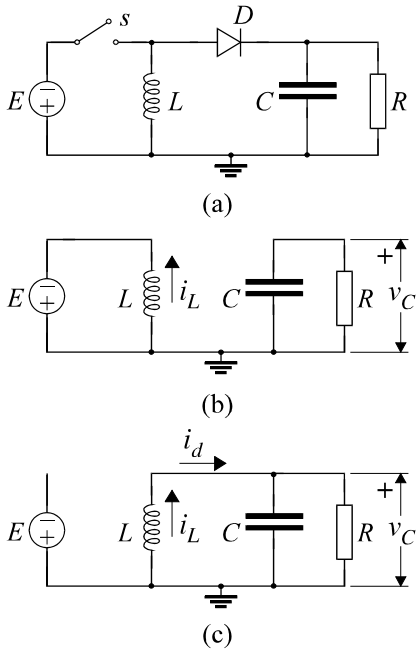

Fig. 5.6: (a) Ideal flyback switching converter. (b) Equivalent circuit for *s* closed and *D* open. (c) Equivalent circuits for *s* open and *D* closed.

Dirac impulse of the inductor voltage would be erased. There cannot be any impulse of the inductor voltage in simulation results, but the Dirac impulse must appear to switch the diode *D*, i.e. to change the value of the control variable *p*. Similar condition happens when *s* is externally closed. Dirac impulse of current appears through capacitor *C*, but it opens diode *D* in the same time instance.

In [Bedr92], special algorithm is developed for simulation of such networks, but with linear elements only. Our switch model enables simulation of such networks using exclusively standard simulation algorithms, and without any restriction in network topology, possible switch states and model linearity. The simulation results for the flyback converter are given in Fig. 5.7. The element values are *E*=1 V, *L*=150 mH, *C*=50 mF, *R*=10 W. The switching period for the switch *s* is 70ms, time when *s* is closed is 30ms, when it is open is 40ms (duty

cycle is $\frac{3}{7}$). These parameters are not optimized from the point of view of circuit performance.

The results show correct transitions of the internally controlled switch *D*. The model is nonlinear, since it uses an iterative procedure for transition from one switch state into another. During this procedure, the existence of Dirac impulse is automatically taken into account, although no special algorithms are used for that. Therefore, the Dirac impulse occurs only in the iterative process, but not in the final solution given in Fig. 5.7, where current i_L and voltage v_C are continuous. However, the Dirac impulse can change the states of other switches in the circuit. The convergence can occur only when all switches in the circuit reach their final state. There is no need to create any special algorithm that would check for the possible occurrence of the Dirac impulses and their influence to the switch states. When the convergence is reached in the whole circuit, all switch transitions are finished and consistent state is obtained, with charge and flux conservation. Details of the switch implementation and analysis of this iterative procedure are given in [Mr~a99].

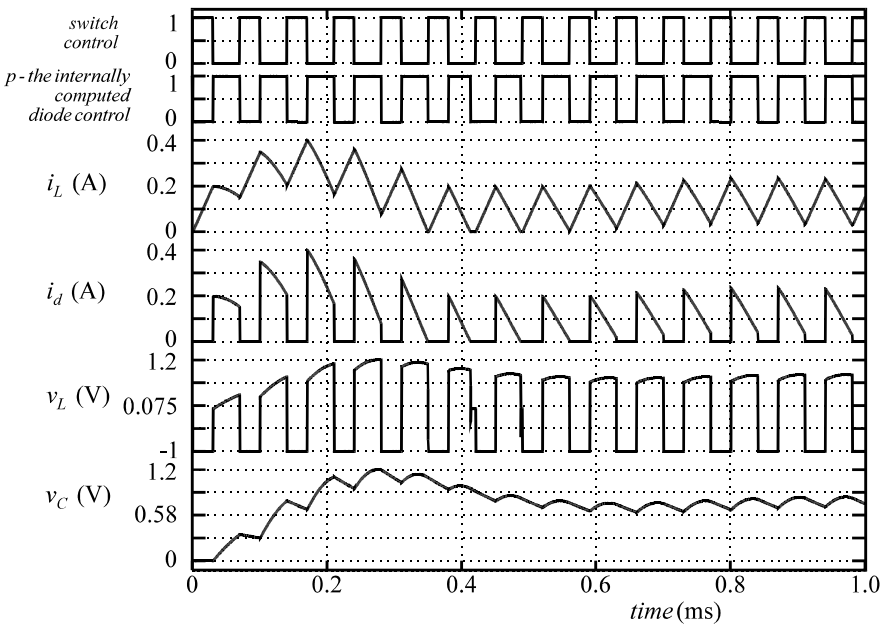

Fig. 5.7: Simulation results for the flyback converter.

5.4. MOSFET modeling using artificial neural network

As shown in section 3.3, modeling of nonlinear analog devices using model cards as static objects has the advantage of separating the nonlinear function and the enclosing process. As long as model class methods accept terminal voltages and return both nonlinear function value and partial derivatives, the actual method implementation is of no importance. We used this property to develop a model class whose methods model MOSFET drain current using artificial neural network. It was shown that an artificial feed-forward neural network may be trained to behave like a nonlinear device, given the sufficient input-output data set, obtained either by measurements or simulation [Lito92, Lito93]. Such a network has as many neurons in the input layer as there are input variables (in our case voltages Vgs and Vds), and one output neuron (Ids). Training has shown that one hidden layer with 10 neurons is sufficient to obtain neural network response with an acceptable error. The results of the training were weights and thresholds associated with the neurons, and they were introduced in the defined model card class as parameters. Once the neural network response method was implemented, the MOSFET model did not differ from the example given in section 3.3, with the identical interface type signature.

The following declaration was used to introduce a model class `annmos`:

```
class annmos {
  private:
    double w[32], t[12], x[50];  // weights, thresholds
    double oj[11], ojg[11];      // intermediate results
    int n, n0, np;               // network dimensions
    int hidden_transfer, outtransfer;   // transfer type
    double hidden_gain, outgain;        // transfer gains
    annmos(int, int, int);       // class constructor
    >annmos();                   // model card preprocessor
    void create_unified_neurodata();    // class unifier
  public:
    double vds_min, vgs_min;     // vds normalization
    double vds_max, vgs_max;     // vgs normalization
    double ids_min, ids_max;     // ids normalization
    double vgsd, vdsd, idsd;     // normalized values
    double Cgd, Cgs, Cgb;        // MOS capacitances
    double Cbd, Cbs;             // junction capacitances
    double type;                 // device polarization
    void neuro_response(double *, double *); // net response
};
```

A subcircuit that defines artificial neural network MOSFET model is defined by the use of structural modeling:

```
module annmos::neuromos ( node drain, gate, source ) {
    vccs e_gm, e_gds;
    cgen iaux;
    // voltage-controlled current sources
    e_gm (drain, source, gate, source);
    e_gds (drain, source, drain, source);
    iaux (drain, source);        // error current
    // capacitances
    cgs (gate, source);
    cgd (gate, drain);
    cds (drain, source);
    action {        // model of the behavior
        process initial { *cgs=Cgs; *cgd=Cgd; *cds=Cds; }
        process per_iteration {
            double inp[3], ok[4];
            double vg, vd, vs, vgs, vds, ids, gm, gds;
            // extract controlling voltages
            vd = drain;   vg = gate;   vs = source;
            vgd = type * (vd - vs);
            vgs = type * (vg - vs);
            // normalize input vector
            inp[INP_VGS] = (vgs - vgs_min)/vgsd;
            inp[INP_VDS] = (vds - vds_min)/vdsd;
            this->neuro_response ( ok, inp );
            ids = ok[1] * idsd + ids_min; // denormalize Id
            gds = ok[2] * idsd / vdsd;     // denormalize gds
            gm = ok[3] * idsd / vgsd;      // denormalize gm
            // update the linear model elements
            iaux->value = type * (ids - gm*vgs - gds*vds);
            e_gm->gm = gm;
            e_gds->gm = gds;
        }
    }
}
```

The simulation of a CMOS inverter composed of two ANNMOS (Artificial Neural Network MOS) devices is illustrated in the Fig. 5.8. Since the nonlinear function that models MOSFET drain current has continuous first derivatives in the entire range of interest (four orders of magnitude), no convergence problems occurred in the transition regions. It should be noted that this modeling method may be used for any nonlinear device or system, given sufficient input-output relation data.

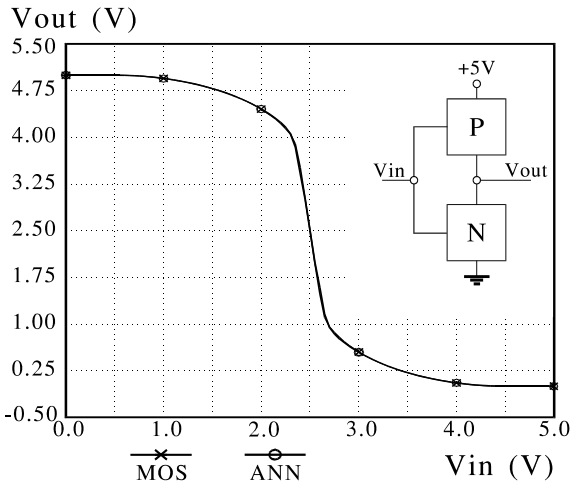

Fig. 5.8: Comparison of the simulation results of a CMOS inverter composed of standard transistor models (MOS) and artificial neural network models (ANN). Two curves evidently match in the whole voltage domain of interest.

5.5. Adaptive fuzzy-logic vehicle engine controller

Fuzzy logic control systems are particularly interesting as mixed-signal systems. Engineers often use general-purpose mathematical packages to develop fuzzy logic control systems. However, those systems eventually end up in hardware, when electronic circuit simulators should be used. Due to AleC++ modeling power, Alecsis is capable of supporting the entire design process, from the conceptual to the final stage. The example of such a system may be an adaptive fuzzy-logic vehicle engine controller, shown in Fig. 5.9.

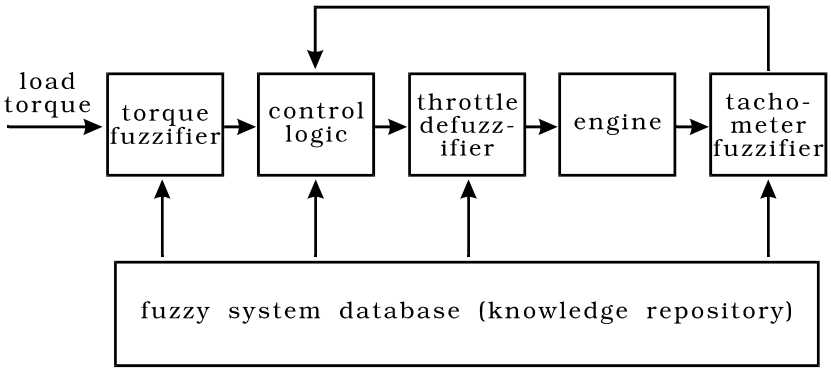

Fig. 5.9: Adaptive fuzzy-logic vehicle engine control system block diagram

The system controls a vehicle engine in order to respond to changes in the road grade [Cox93]. The engine speed is monitored using a tachometer. In order to solve the control problem using the fuzzy-logic approach, the tachometer readings and the road grade are first fuzzyfied. This information is used to produce a fuzzyfied engine throttle movement value in the control logic block. The exact (crisp) control value is obtained in the defuzzyfication module, and then applied to the engine. As expected, the entire system is parameterized by creating a new model class, containing data about fuzzy regions, domain knowledge in the form of a fuzzy associative matrix, rule weights and so on. Connections between the modules are modeled using variables of type `flow` for crisp values, and structures for fuzzy values. The entire system is self-adaptive, i.e. capable of responding to long-range changes in the environment. The behavior of all of the modules is implemented as model class methods, including the self-adaptation mechanism. The vehicle engine was modeled using an ordinary differential equation by means of AleC++ `eqn` statement.

The first step in modeling for Alecsis is to create a new class that describes resources needed in the simulation:

```
class fuzzy {
    int ntach;    // number of tachometer fuzzy values
    int nlt;      // number of load torque fuzzy signals
    int ntas;     // number of throttle mov. fuzzy values
    FUZZY_VALUE tach[TACHSIZE]; // tachometer fuzzy logic system
    FUZZY_VALUE torq[LTSIZE]; // load torque fuzzy logic system
    FUZZY_VALUE tas[TMSIZE];  // throttle action fuzzy log. sys.
    double tcmin, tcmax;// tachometer range
    double trqmin, trqmax;     // load torque range
    double tamin, tamax;// throttle action range
    int fam[LTSIZE][TACHSIZE];// fuzzy assoc. memory (knowledge)
    int center_of_response[2];// steady-state location
    double weights[LTSIZE][TACHSIZE];  // FAM weights matrix
    void fuzzy(int);           // class constructor
    void ~fuzzy(int);          // class destructor
    double engine_response;    // engine reaction
  public:
    double memf(FUZZY_VALUE*,double,double); // membership func.
    void evaluate_output(double*,double*,double*,int);// mapping
    double integrate(double*); // evaluation of centroid
    void update_weights();     // auto-adaptation of weights
};
```

After the definition of the model class, an unlimited number of model cards of that class may be constructed. An example may look like this:

```
model fuzzy::speed_cont {
    ntach=5;   nlt=4;      ntas=5;     tcmin=0.1;   tcmax=8.0;
    trqmin=0;  trqmax=40;  tamin=-60;  tamax=60;
    // tachometer fuzzy value system coordinates (feedback)
    tach = { { "very_slow", { 0.1,  0.1,  0.4,  0.8 } },
             { "slow",      { 0.5,  1.65, 1.65, 2.8 } },
             { "optimal",   { 2.0,  3.25, 3.25, 4.5 } },
             { "fast",      { 3.2,  4.7,  4.7,  6.2 } },
             { "very_fast", { 5.5,  7.0,  8.0,  8.0 } } };
    // load torque fuzzy value system coordinates (feed forward)
    torq = { { "zero",              {  0,    0,  2.5, 10 } },
             { "small_positive",    {  5, 12.5, 12.5, 20 } },
             { "moderate_positive", { 15, 22.5, 22.5, 30 } },
             { "large_positive",    { 25, 32.5,   40, 40 } } };
    // throttle action fuzzy value system coordinates (output)
    tas = { { "LN", { -60, -60, -45, -30 } },
            { "SN", { -40, -20, -20,  -2 } },
            { "ZR", { -10,   0,   0,  10 } },
```

```
            { "SP", {   2,  20,  20,  40 } },

            { "LP", {  30,  45,  60,  60 } } };
    // fuzzy associative memory (knowledge repository)
    fam = { { LP, SP, ZR, SN, LN },
            { LP, SP, ZR, ZR, SN },
            { LP, SP, SP, SP, ZR },
            { LP, LP, LP, SP, SP } };
    // initial equilibrium center on the control surface
    center_of_response = {Optimal, Zero };
    // initial rule contribution weights - all rules are equal
    weights = { { 1, 1, 1, 1, 1 },
                { 1, 1, 1, 1, 1 },
                { 1, 1, 1, 1, 1 },
                { 1, 1, 1, 1, 1 } };
}
```

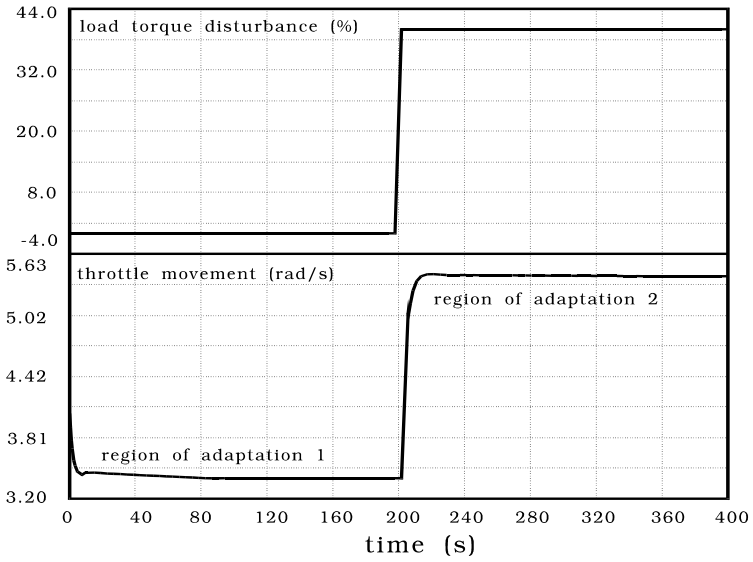

Fig. 5.10: Vehicle engine control system response to rapid change in the road grade

Fig. 5.10 shows the system response to a rapid change in the road grade. Two distinct regions exist in the response curve: one, that represents the primary response, and another, where the system slowly adjusts the rule weights to move the center of the response to a different location. This effect is shown in the weight surfaces in the Fig. 5.11. The center-of-response displacement is clearly visible on the surface contour lines.

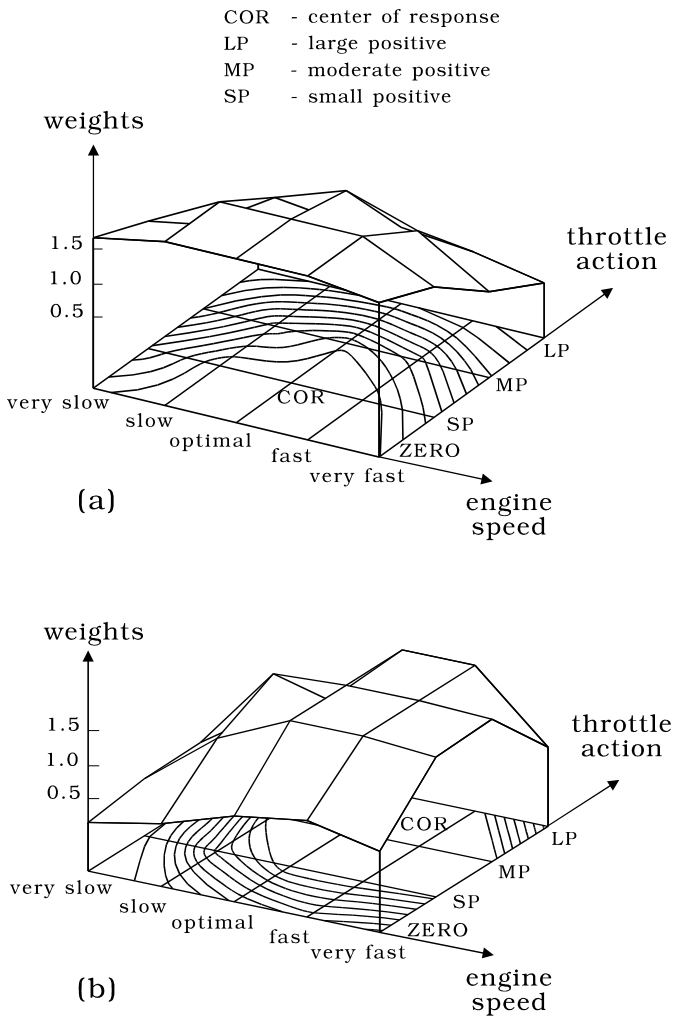

Fig. 5.11: Weight surfaces before (a) and after (b) the road grade change. The center of response has visibly moved towards the new equilibrium point.

5.6. Continuous time control system simulation

When systems are described on a higher level of abstractions, block diagrams can be used for their representation. Control systems are often represented using such description. A transfer function in *s*-domain of one subsystem (block) can be represented as a rational function:

$$H(s) = \frac{D(s)}{N(s)} = \frac{b_0 + b_1 s + \ldots + b_m s^m}{a_0 + a_1 s + \ldots + a_n s^n} \qquad (5.2)$$

Such expressions can be realized as shown in Fig. 5.12, when the control form representation is used.

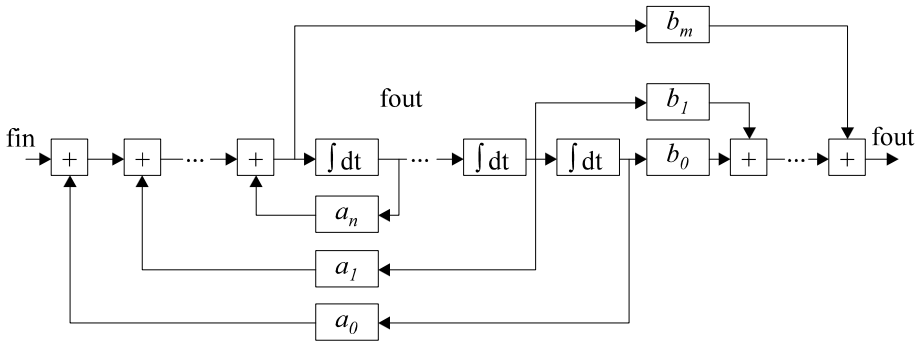

Fig. 5.12: Control form representation.

When writing transfer function module, we are using modules that describe smaller blocks in Fig. 5.12. For instance, integrator block is represented through:

```
module integral (flow fin, fout) {
   action (double w=1.0) {
      process per_iteration {
         eqn fout: { fout } - w * idt { fin } = 0;
      }
   }
}
```

The command `clone` was used to model an array of integrators, as well as gain stages that create inputs to the adders. This is contained inside the module `transfer` (not given here), representing the block scheme from the Fig. 5.12.

As an example of continuous-time system simulation the response of a pulse compressing allpass filter will be evaluated. The transfer function of the circuit is given by

$$T(s) = \prod_{i=1}^{6} \frac{s^2 - 2\sigma_i s + \left(\sigma_i{}^2 + \omega_i{}^2\right)}{s^2 + 2\sigma_i s + \left(\sigma_i{}^2 + \omega_i{}^2\right)},$$

$(\sigma, \omega)_i$ being the pole/zero coordinates as given in Table 5.1.

Table 5.1:

i	σ_i	ω_i
1	0.051690	0.568976
2	0.057089	0.646074
3	0.064608	0.731975
4	0.076094	0.830426
5	0.096704	0.948449
6	0.147276	1.098074

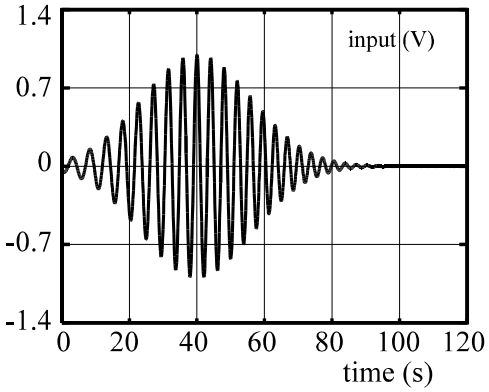

Fig 5.13.a: The input signal

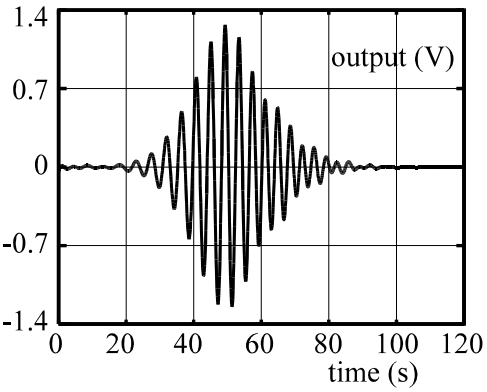

Fig 5.13.b: The output signal

The input signal is frequency modulated and gaussian shaped:

$$v_{in} = e^{-at^2} \cos\left(\omega_0 t + bt^2\right),$$

where ω_0 = 1.52344, a = 0.11033215 and b = 0.25794107 [Laz72], given in Fig 5.13.a.

The output (amplified and monochromatic) signal as obtained by simulation is depicted in Fig 5.13.b.

Here, again, the `clone` command was used in order to replicate the basic second order allpass cell six times.

5.7. Nonlinear magnetic circuit modeled using artificial neural network

Direct current magnets have found a wide range of applications, as actuating elements in devices with automatic control, in precision mechanics, etc. Latest applications of these magnets have set more rigorous requests with regard to increase of the switching speed and dimension miniaturization. It is very important to model and simulate electromagnets, in order to optimize their parameters. Especially important is transient analysis, where the goal is usually to find the optimal waveform of the input voltage in order to obtain fast switching of the armature, but to avoid damage of the contacts caused by collisions.

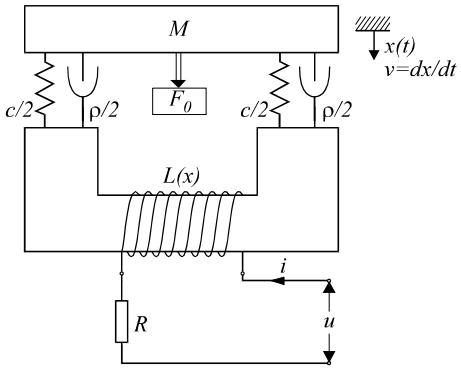

Fig 5.14: An electromagnetic circuit

Schematic representation of a DC magnet is shown in Fig. 5.14. Position of the electromagnet is determined by the equilibrium of mechanical and magnetic forces:

$$F_{mag} = F_{mech} \tag{5.4}$$

Mechanical force is a sum of four components. These may be expressed as shown in Table 5.2.

Notation used here is: M for mass, c for spring constant, ρ for friction resistance.

Table 5.2: Mechanical forces acting on the armature.

Mass	Spring	Friction	Constant force
$F = M \cdot \frac{dv}{dt}$	$\frac{dF}{dt} = c \cdot v$	$F = \rho \cdot v$	$F = F_0$

Total mechanical force is then:

$$F_{mech} = M \cdot \ddot{x} + \rho \cdot \dot{x} + c \cdot x + F_0 \tag{5.5}$$

The value of the magnetic force depends on electrical quantities. Electrical part of the device can be modeled as:

$$u = R \cdot i + \frac{d\psi}{dt} \tag{5.6}$$

where R represents ohmic resistance of the coil, and ψ is the magnetic flux. The flux is determined by the current through the coil and the size of the air gap between the movable armature and the magnet core.

$$\psi = f(i, x) \tag{5.7}$$

Magnetic force can be than calculated as:

$$F_{mag} = \frac{\partial E_{mag}}{\partial x} = \frac{\partial}{\partial x} \int_0^i \psi \cdot di = g(i, x) \tag{5.8}$$

where E_{mag} denotes electromagnetic energy in the air gap.

The equilibrium equation (1) can now be written as:

$$g(i, x) = M \cdot \ddot{x} + \rho \cdot \dot{x} + c \cdot x + F_0 \tag{5.9}$$

Equations (5.6) and (5.9) represent the model of the magnet that should be implemented in an HDL. Unfortunately, function that determines flux is, as is already mentioned, usually very difficult to obtain in a closed form. An artificial neural network (ANN) can help solving this problem. We used ANN shown in the Fig. 5.15 to approximate flux as a function of *i* and *x*. Moreover, neural network can be used to calculate directly *g(i,x)*, i.e. the magnetic force. Force is the function of the same inputs *i* and *x*, and the same network calculates both values. For that reason, network in Fig. 5.15 has two output neurons. Both values are necessary for implementation of the model in the simulator (equations (5.6) and (5.9)).

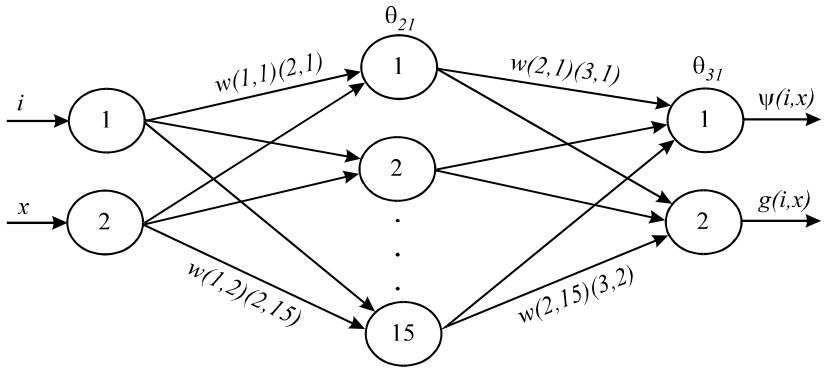

Fig. 5.15: ANN used in modeling magnetic characteristics

As mentioned in section 3.2, AleC++ have special operators for description of first and second order time derivatives. The latter one was developed particularly for description of mechanical systems, since second order differential equations are often in use there. For that reason, eqn. (5.9) can be described nearly as it is given in the text.

```
main_equation: process per_moment {
   eqn x:  -{Fmag}  +M*d2dt2{x}  +RO*ddt{x}  +c*{x} = -F0;
}
```

For the voltage excitation the step function is used. Its amplitude was 24V. All variables (x(t), v(t) and a(t)) were considered zero for t=0. In Fig. 5.16(a) the simulation results are given. As may be seen, the movable part of the core eventually reaches its goal with significant velocity. These results are to be compared with measured ones given in Fig. 5.16(b).

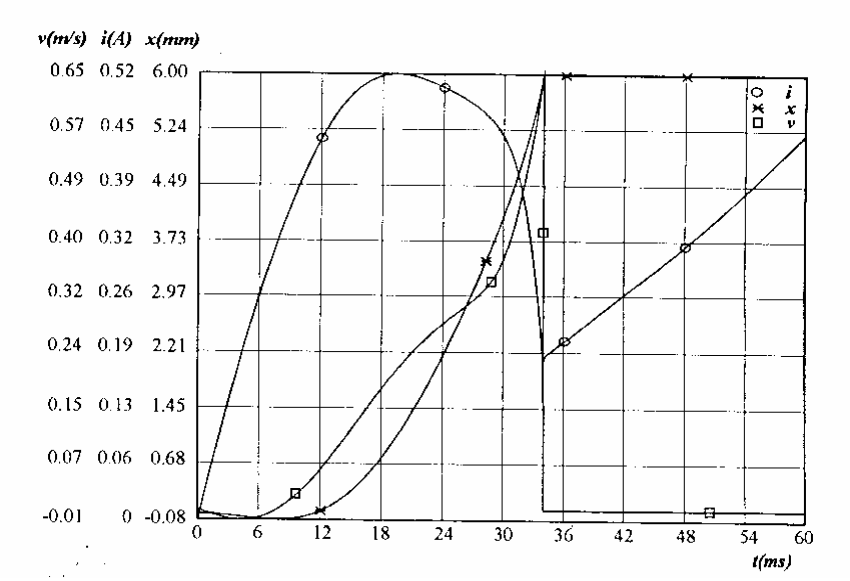

(a)

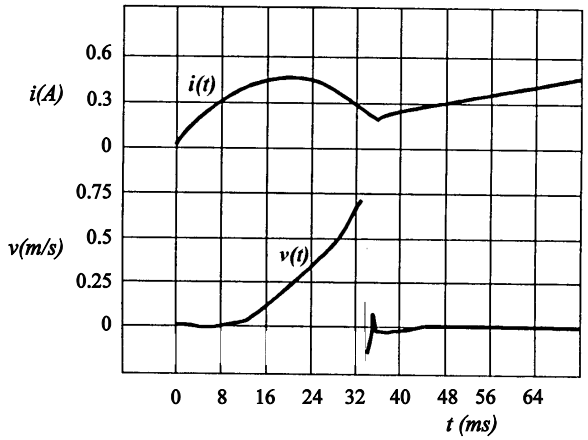

(b)

Fig. 5.16: (a) Simulation results. (b) Measured characteristics.

5.8. Pressure sensing system

AleC++ is a HDL created as a superset of the standard programming language. Its programming features are very helpful in defining complex models. In this example we have used them to model devices with distributed parameters.

In Fig. 5.17, a micro-electro-mechanical pressure sensing system is shown. A rectangular capacitor membrane is deformed when pressure is applied. Membrane deformation is modeled using a partial differential equation [Timo59]. That equation can be discretized and represented as a system of ordinary differential equations. Discretization is performed in the `for` loop in the `action` block of the module. That `for` loop must be in the structural process (types of process synchronization are given in the section 3.2), since the structure of the system of equations must be defined before the simulation, and the structural processes are performed before the actual simulation starts.

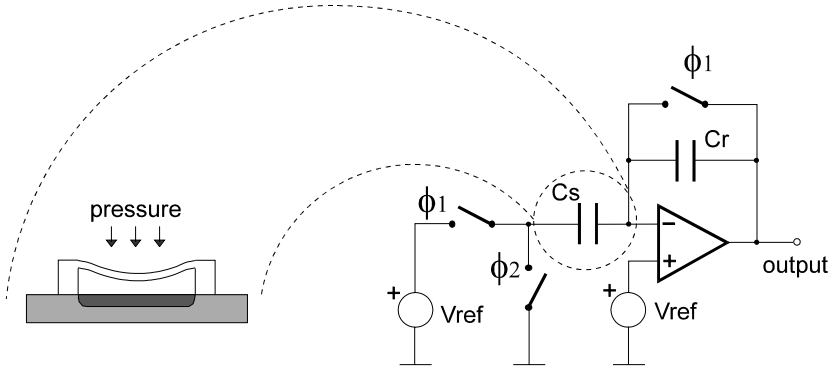

Fig. 5.17: Micro-electro-mechanical capacitive pressure sensing system.

The time-domain simulation results are given in the Fig. 5.18. The spatial displacement of the membrane for one time instant of time-domain simulation is given in Fig. 5.19. It is interesting to note that the graphical postprocessor that is used to create all time-domain simulation results is also a class described in AleC++ language and stored in the library. For spatial drawings, as given in Fig. 5.19, a new class is defined in AleC++, derived from the class for standard, time-domain waveforms. In this way, we did not have to write a new graphical postprocessor for this purpose. Functions from the base class are used, just some new had to be added to the derived class. Both the time-domain simulation results and the spatial drawings can be viewed during the simulation run.

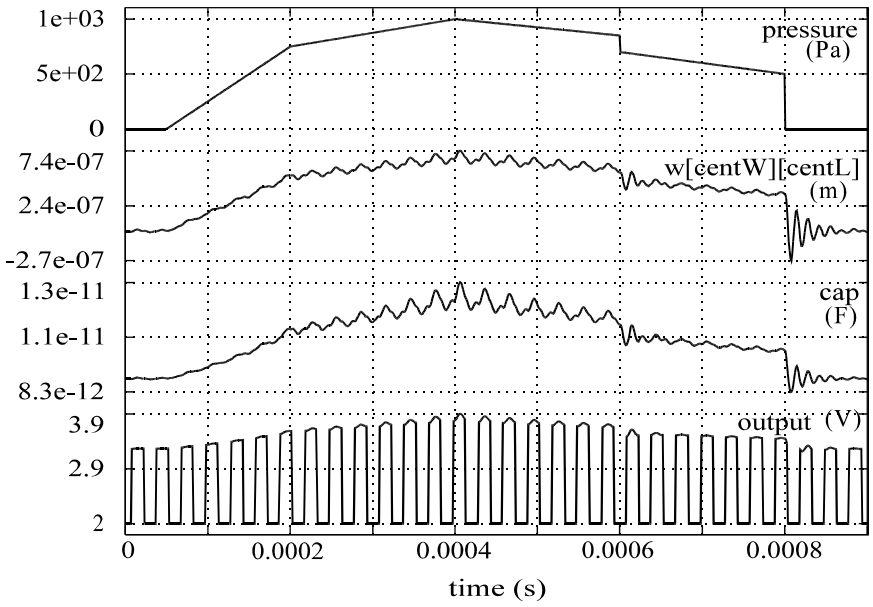

Fig. 5.18: Time-domain simulation results for the system given in Fig. 5.17. Traced signals are pressure, displacement of the pressure sensor center, sensor capacitance, and the output voltage.

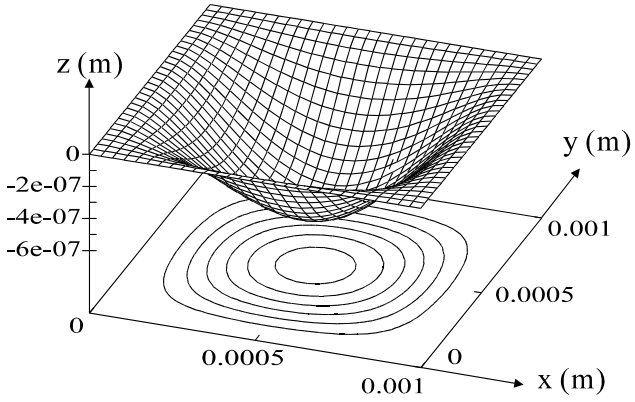

Fig. 5.19: Displacement of the sensor membrane for simulation time instant 0.0004s in Fig. 5.18.

5.9. Thermoelectrical simulation

In many microsystems and microelectronic circuits thermal effects have significant importance. Spatial distribution of the temperature on a chip should be simulated, together with electronic subsystem. The coupling is bidirectional, as electronics is influenced by the temperature, and electronic components represent heat sources.

Thermoelectrical simulation is performed in Alecsis using finite element (FE) method for spatial discretization. The user defines the geometry and placing of the components on the wafer by using commercial FE software with meshing capabilities. The strength of the method is in the fact that FE discretization can accurately describe the physical laws on irregular shapes with irregular mesh. The system of equations is extracted into the form applicable to analogue simulators. Afterwards, the electronic system or components described on higher level of abstraction are defined and coupled with thermal FE modules. Alecsis is employed to solve a system, assembled from particular element models previously programmed as libraries in AleC++.

The quality of the approach can be described on the flow sensor based on anemometry principle (system in Fig. 5.20, similar to [Jime98]). The heating resistor is employed for generating thermal gradient in the region of interest (wire, cantilever, bridge). The temperature difference between the referent and the heated position is proportional to the velocity of flow, since the flow disturbs the distribution of thermal gradients. It is a fluidic-thermal-electric system and requires simultaneous treatment of all participating physical domains.

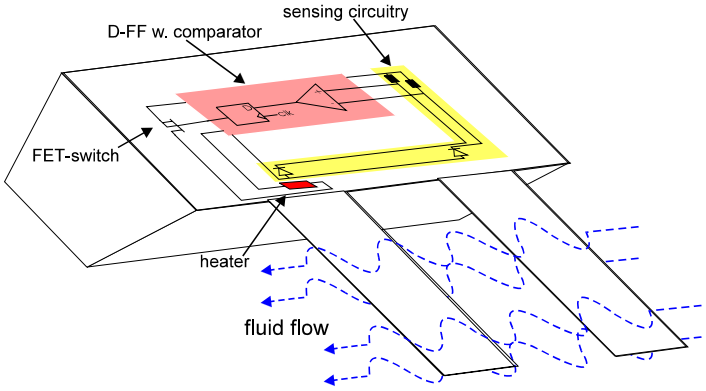

Fig. 5.20: The flow sensor with the circuitry.

The placement of the components is shown in Fig. 5.20. It describes the circuitry for defining constant average temperature difference between the heater and the reference. The fluid influences the thermal flow, and that flow is measured by the temperature-dependant diodes.

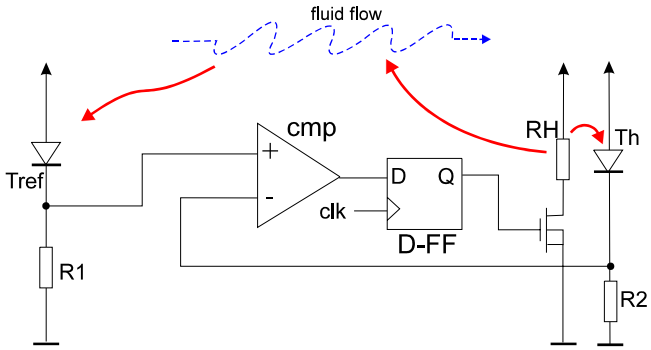

Fig. 5.21: Main thermal flows in the flow sensor.

This system defines a sigma-delta converter of the first order with the low-pass feedback incorporated in the thermal system (Fig 5.21). The FET transistor is switched depending on the temperature difference between the heater and the reference. The frequency of the switching is a measure of the flow velocity.

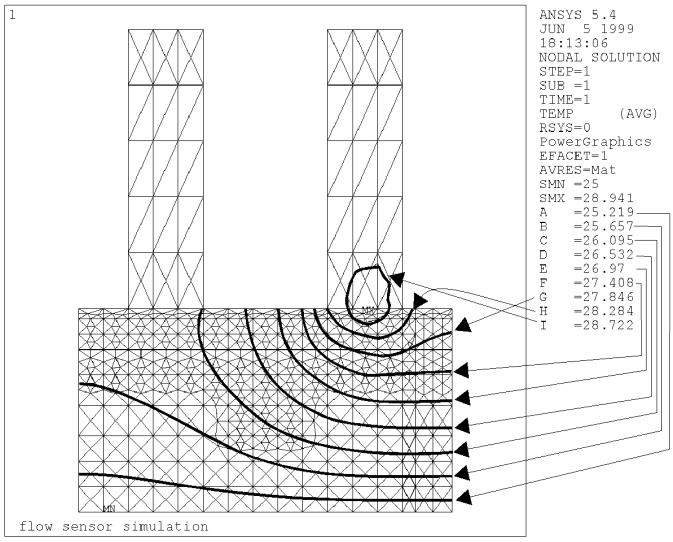

Fig. 5.22: Temperature distribution on the chip.

The ANSYS v5.4 results for 2D thermal simulation with emphasized isotherms are shown in Fig. 5.22. Comparison with Alecsis results for the same thermal system shows relative error smaller than 0.002%. The 2D model was somewhat simplified. The bottom part of the structure in Fig. 5.22 has fixed temperature, which presumes the connection with an ideal sink. The system is modeled as adiabatic in z-plane, i.e. there is no heat transport in the direction of the z-axis.

Alecsis transient simulation results of the coupled electro-thermal system are shown in the Fig. 5.23. Traced signals are the heater temperature, the temperature of the cantilever close to the heater, the reference temperature, the measured fluid velocity, and the clock signal. Results show change of the frequency of the heat pulses with the change of the fluid flow velocity.

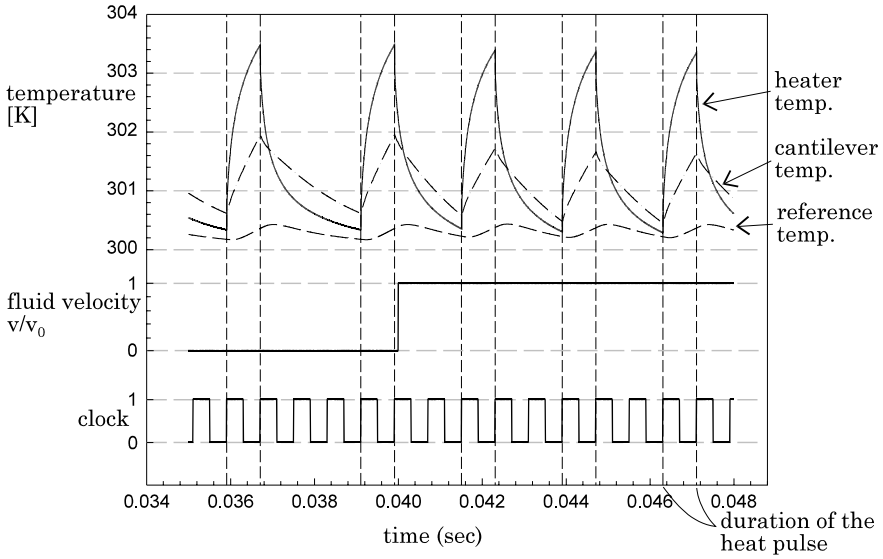

Fig. 5.23: Transient results for the behavior of the flow.

More details about electrothermal simulation in Alecsis can be found in [Jako99].

5.10. Digit-serial 8-bit systolic array multiplier

Like VHDL, AleC++ does not favor any logic value system. The logic value system and appropriate lookup tables, overloaded logic operators, basic logic gates, bus resolution functions, etc., can be described in AleC++ and conveniently stored in the library and retrieved when needed.

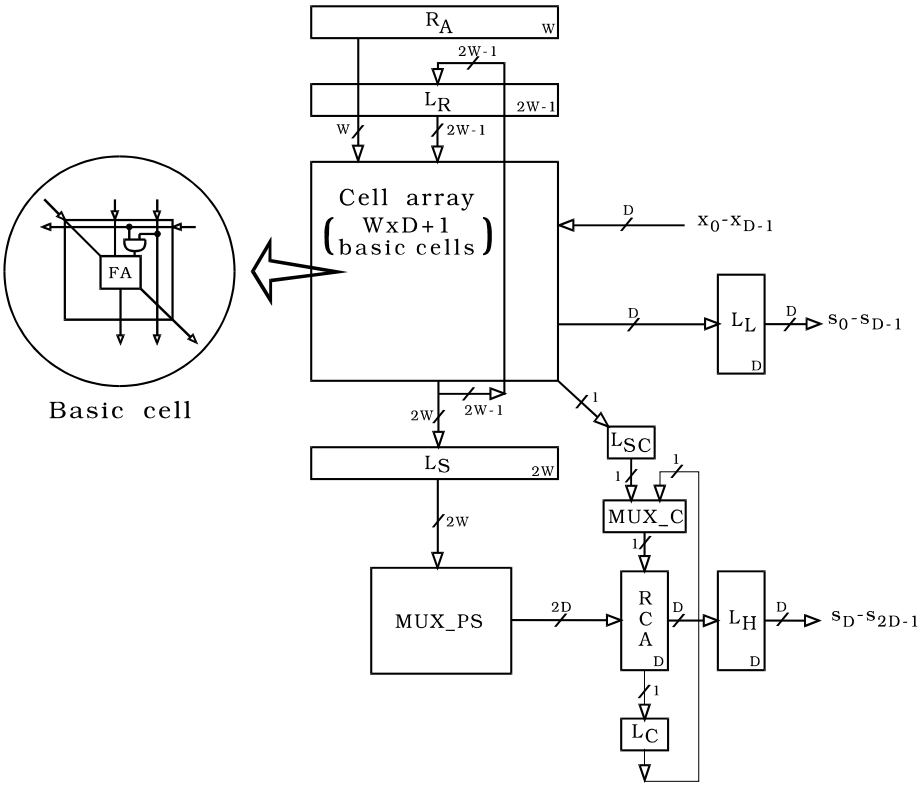

Fig. 5.24: Block diagram of digit-serial semi-systolic multiplier: R_A - register for the first operand of multiplication; L_R and L_S - latch arrays storing partial products; MUX_C - multiplexer 2 to 1; MUX_PS - multiplexer 2W to 2D; L_{SC} and L_C - latches; RCA - ripple carry adder; L_L and L_H - latch arrays storing lower and higher portions of the result; FA - full adder.

The digit-serial multiplier shown in the Fig. 5.24, the building element of more complex semi-systolic architectures [Mile95, Mile96], is simulated using a pre-compiled library developed to emulate the HILO logic simulator [Harr85]. The multiplier is composed of basic processing elements that communicate locally and work in synchronization. The first operand of the length W is available in parallel in register R_A, while the second (X) is fed in digit-by-digit, where the number of bits in a digit is marked as D. The multiplier operates in two phases: in the first phase the lower portion of the product is generated at the outputs s_0-s_{D-1}, while the other half is available in the second phase at the outputs s_D-s_{2D-1}.

Let us illustrate the multiplier modeling by showing the simplified model of full adder, which is part of the systolic array basic element, as shown in Fig. 5.20. Firstly, the model class `fadd` is defined.

```
// model parameters defined with min, typical and max value
typedef double param[3];
// different delays from inputs to outputs, direction flags
#      define FROM_AB             0
#      define FROM_CIN            1
#      define TO_SUM              0
#      define TO_COUT             1
#      define TAKE_MAX_DELAY      -1
// full adders model class
class fadd {
       param delay01[2][2];// rising edge propagation delay
       param delay10[2][2];// falling edge propagation delay
       fadd();
       >fadd();
  public:
       // delay function
       double ADDdelay (three_t, three_t, int, int);
       friend module fa;
};
```

Full adder module is described with the following code.

```
module fadd::fa (fift_t in a, b, c_in;
                 fift_t out sum, c_out) {
  action {
    process (a, b, c_in) {
      three_t a3, b3, c_in3, sum_result, cout_result;
      int from_in;
                   // detect active input


      if((a->event || b->event) && c_in->stable)
```

```
            from_in = FROM_AB;

          else if( c_in->event && a->stable && b->stable)
            from_in = FROM_CIN;
          else {        // simultaneous event at (a or b)/c_in
            warning(
               "fadd::fa - simultaneous (a or b)/c_in change");
            from_in = TAKE_MAX_DELAY;
          }
                        // convert input states to three_t
          // log. operations are not held in HILO's 15-st. log.
          // system (fift_t), but in 3-state system (three_t).
          a3 = Con15to3[a];
          b3 = Con15to3[b];
          c_in3 = Con15to3[c_in];
                        // evaluate logic function
          sum_result = a3 ^ b3 ^ c_in3;
          cout_result = (a3 & c_in3) | (a3 & b3) | (b3 & c_in3);
          sum <- Con3to15[sum_result] after
                 this->ADDdelay(sum_result, Con15to3[sum],
                                            from_in, TO_SUM);
          c_out <- Con3to15[cout_result)] after
                 this->ADDdelay(cout_result, Con15to3[c_out],
                                            from_in, TO_COUT);
        } // process (a, b, c_in)
      } // action
    } // module fadd::fa ()
```

The above code is part of mentioned Alecsis library for HILO emulation. In order to use the module `fa` in multiplier description for simulation, user has to connect the library file and to define its model card. One particular model card for a full adder module is as follows.

```
    model add15::fa_1 { // {min value, typ value, max value}
      delay01[FROM_AB][TO_COUT] = {0.2ns, 0.5ns, 1.0ns};
      delay10[FROM_AB][TO_COUT] = {0.3ns, 0.6ns, 1.5ns};
      delay01[FROM_CIN][TO_COUT]= {0.3ns, 0.5ns, 1.3ns};
      delay10[FROM_CIN][TO_COUT]= {0.3ns, 0.6ns, 1.5ns};
      delay01[FROM_AB][TO_SUM]  = {1.3ns, 2.4ns, 5.6ns};
      delay10[FROM_AB][TO_SUM]  = {0.9ns, 2.2ns, 6.0ns};
      delay01[FROM_CIN][TO_SUM] = {0.5ns, 0.9ns, 2.0ns};
      delay10[FROM_CIN][TO_SUM] = {0.4ns, 0.9ns, 2.7ns};
    }
```

The multiplier is simulated at gate level, using generic structures that enabled the word length to be passed as an action parameter. An example of the simulation results for the configuration with W=8 and D=4 is shown in the Fig. 5.25. The entire circuit contains more than 500 gates modeled with more than 1000

concurrent processes, while around 25000 events were handled during the simulation. It took 4.76 CPU seconds to simulate the circuit using Alecsis implementation on Hewlett-Packard Series 9000/375 platform with Motorola MC68020 processor. The simulation results obtained using HILO logic simulator were identical. Unfortunately, HILO was implemented on a different platform and simulation times were not comparable.

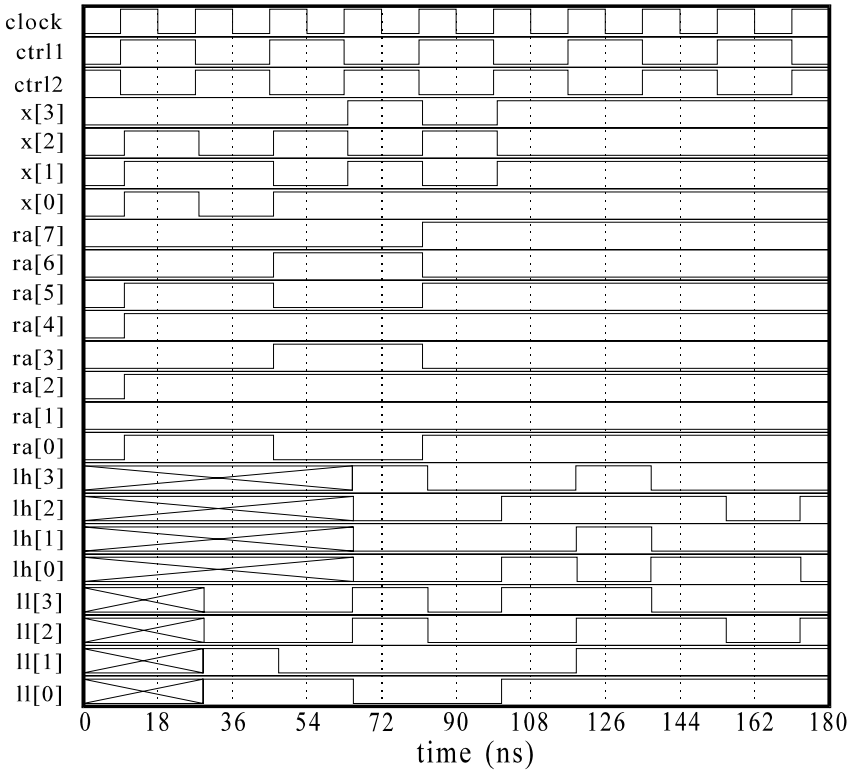

Fig. 5.25: Example of simulation results for 8-bit configuration of the multiplier from Fig. 5.24: clock, ctrl1 and ctrl2 are global control signals; x[0] - x[3] are inputs for second operand; ra[0] - ra[7] are R_A outputs (first operand); lh[0] - lh[3] are the outputs of L_H; ll[0] - ll[3] are the outputs of L_L.

5.11. LAN Ethernet network simulation

While the previous example shows Alecsis use in gate-level logic simulation, this one will illustrate its capabilities at higher levels of abstraction. Using signals typed as classes, it is possible to create complex inter-process communication. Fig. 5.26 shows Local Area Network (LAN) modeled using AleC++ discrete-event simulation constructs. Each workstation is represented as an autonomous concurrent process with its own activity pattern. LAN cable segments between stations are modeled as simple bi-directional buffers that pass information with some transport delay proportional to the cable length. After non-deterministic idle periods calculated using the uniform random distribution, the stations attempt to send their frames, according to CSMA/CD protocols [Watk93, Schw87]. After sending the frame, the station monitors the line for the specified period (*2*slot_size*), and then compare the original and the frame on the line. If they are not the same, the collision took place, and the frames are scheduled for retransmission after a period calculated using *binary exponential backoff* algorithm. According to CD (Collision Detection) strategy, the station is capable of truncating the corrupted frame without waiting *2*slot_size* period in case of collision.

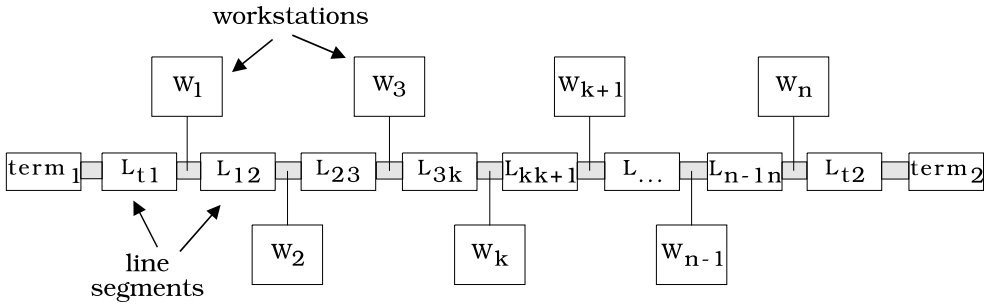

Fig. 5.26: Schematic of an abstract LAN Ethernet network

The workstation model in AleC++ is as follows.

```
enum StationState { NormalState, CollisionState };
```

```
module LAN::workstation(frame inout lan_port) {
    action (int id, const char *ws_name) {

        process {
            frame last_frame;
            double last_sent = 0.0;
            StationState ss = NormalState;
            int ntrials = 0;
            if (ss == NormalState) {
              wait for idle_period();
              last_sent = now;
              if ( !lan_port.status (FreeLine) )
                wait lan_port while
                                !lan_port.status(FreeLine);
            }
            last_frame.stamp(NormalFrame, id,
                           receiver(id, nst), now, ws_name);
            lan_port <- last_frame;
            last_sent = now;
            wait lan_port for listen_period();
            if ( last_frame != lan_port ) {
              if (ss == NormalState) {
                ntrials = 0;
                ss = CollisionState;
              }
              ntrials++;
              if(ntrials > max_trials() ) {
                ss = NormalState; // discard frame
                ntrials = 0;
              } else {
                lan_port <- frame(NoiseBurst, now);
                wait for burst_period();
                lan_port <- frame(FreeLine, now);
                wait for retrans_period(ntrials);
              }
            }
            else {  // successful transmission
              ss = NormalState;
              lan_port <- frame(NoiseBurst, now);
              wait for burst_period();
              lan_port <- frame(FreeLine, now);
              last_frame.stamp(FreeLine,0,0,now,ws_name);
            }
        }
    }
}
```

The complete modeling procedure for this problem is explained in [Maks95].

As in all previous examples, workstation modules are parametrized using model card class. That gives an opportunity to create model cards of real

workstations, with different idle times and activity patterns. Fig. 5.27 shows the simulation results of an abstract LAN Ethernet network with 50 workstations interconnected with 5m cable segments. The stations were idle from 0 to 10ms, while the simulation covered 0.2s time period. The curve represents number of stations waiting to transmit their frames due to the occupied line. All the stations were capable of gathering the statistical data about network performance. Post processing of those data carried out in a process synchronized using implicit signal `final` showed that 712 frames were sent successfully, while 1319 frames were re-transmitted due to a collision. The total transmission delay was 2.43s, average delay per station 47.6ms, and average delay per frame 3.47ms.

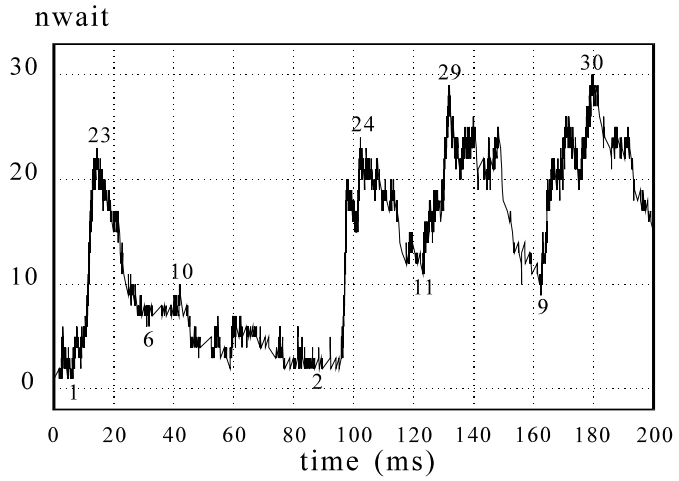

Fig. 5.27: Simulation results of the LAN Ethernet network with 50 workstations. The curve represents number of stations waiting to transmit their frames due to occupied line.

As the next example, the Ethernet bridge modeling and simulation will be considered.

The Ethernet bridge, as shown in Fig. 5.28, interconnects network segments. The network layer as well as all other (transport, session, presentation and application) layers are not affected by the bridge, so that the bridge is totally transparent to the user. Two main functions of the bridge are: filtering traffic (bridges provide for a filtering component to improve network performance) and bridging media. (Bridges frequently interconnect different networks. These networks are often Ethernet or token ring. The bridges merely duplicate all signals originating from all source networks and send them to other networks.)

In the example considered here, the bridge has two LAN-boards because it interconnects two segments. The received frame on one board (`port1`) has to be transferred by the bridge to another segment via appropriate LAN-board (`port2`). In operation mode, the bridge may be in one of the following five states:

1. **NormalState** - in this state the bridge waits to receive frames

2. **TransmisionState1** - in this state bridge attempts to send a frame to port 1

3. **CollisionState1** - in this state, after collision, the bridge resends the frame to port 1

4. **TransmisionState2** - in this state the bridge attempts to send a frame to port 2

5. **CollisionState2** - in this state, after collision, the bridge resends the frame to port 2.

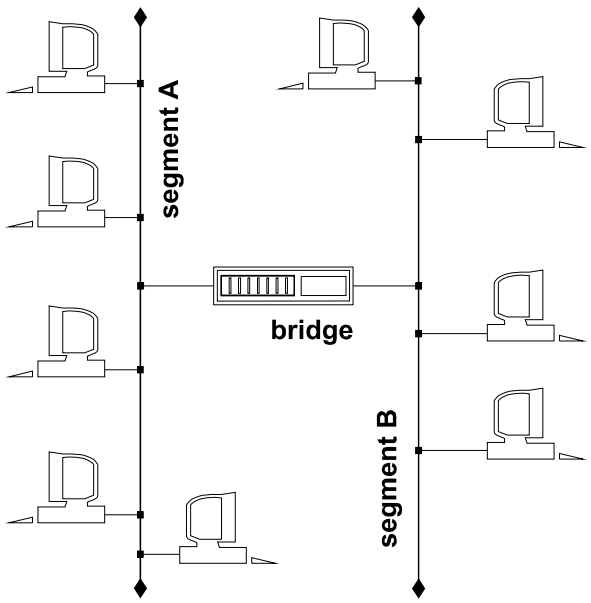

Fig. 5.28: Ethernet LAN with a bridge

The state-transition diagram used for modeling is presented in Fig. 5.29 in a form of an oriented graph. For simulation purposes, in addition to the network topology and functionality, the time properties for every network element and delay times for every state transition should be given. The next AleC++ code describes a bridge in a computer network.

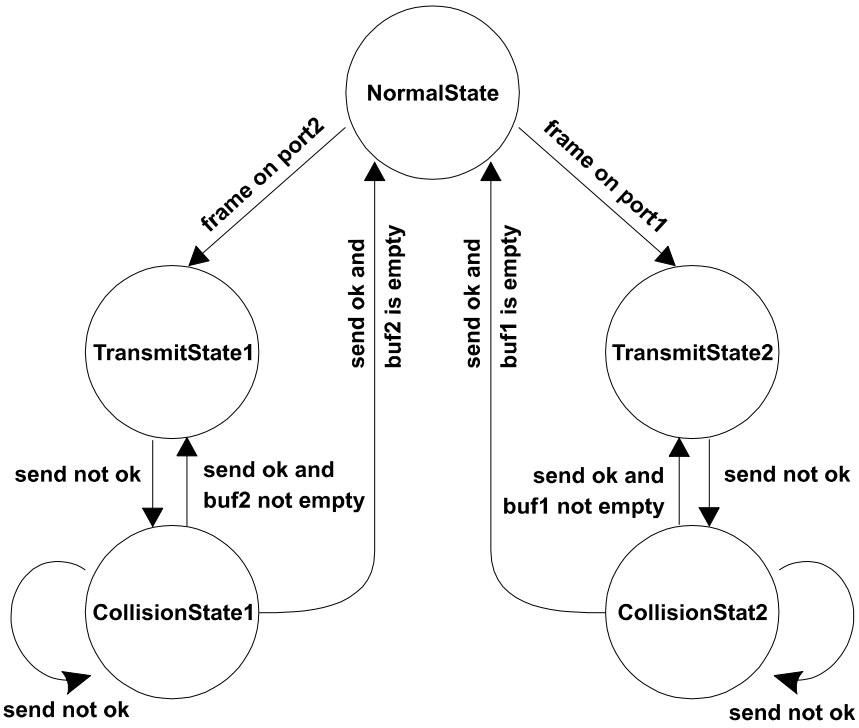

Fig. 5.29: State-transition diagram used for bridge modeling

```
//libr. lanb contains modules: cable,workstation,bridge,...
library lanb;
// model cards for stations and bridge
model LAN::sgi_indigo {
  frame_size=256; max_retrans=16; idle_time=IdleTime;
}
model LAN::hp9000 {
  frame_size=256; max_retrans=16; idle_time=IdleTime;
}
model LAN::bridge2 { frame_size=256; max_retrans=16; }
...


root module net_with_bridge ( ) {


  // declarations of workstations, cables and bridge
  module workstation w1, w2, ... ;
  cable c_1, c_2,  ... ;
```

```
    module bridge b1;
    ...
    // signal declarations
    signal cable_t w1_port={FreeLine}, w2_port={FreeLine};
    signal cable_t b1_port1={FreeLine}, b1_port2={FreeLine};
    signal cable_t term_1={FreeLine}, term_2={FreeLine};
    ...
    // instantiation
    w1(w1_port)
      {ws_name="indigo"; id=5; nst=numst; model=sgi_indigo;}
    w2(w2_port)
      {ws_name="hp";     id=6; nst=numst; model=hp9000;    }
    b1 (b1_port1, b1_port2)
      { bg_name="bg301"; id=20; model=bridge2;}
    c_5 (w1_port, w2_port)  cable_delay = Ldelay(4.0_meter);
    c_2 (w1_port, b1_port1) cable_delay = Ldelay(5.0_meter);
    c_6 (w2_port, term_2)   cable_delay = Ldelay(0.1_meter);
    ...
    timing { tstop = 13*IdleTime; }
    ...
  }
```

As simulation result, statistics are obtained related to all the stations, the bridge (see Table 5.3), and overall network. Table 5.3 contains two kinds of data: number of frames is given in the first five rows, while the last two rows represent delays caused by the data transfer through the bridge.

Table 5.3: Bridge activity statistics

	Bridge	Port 1	Port 2
received frames total	60	43	17
for transmission	25	18	7
successful	23	16	7
unsuccessful	2	2	0
repeated	14	12	2
total delay [s]	0.0062464		
mean delay [s/frame]	0.0001041		

5.12. Successive-approximation 8-bit serial A/D converter

This example represents the ability of Alecsis to support the top-down hierarchical refinement of complex hybrid systems. Fig. 5.30 shows the block diagram of a successive-approximation serial A/D converter. The converter can serve as a mixed signal simulation benchmark for the following reasons:

- the system contains analog (comparator), digital (control and weighting logic, shift register), and mixed-signal subsystems (sample and hold circuit, D/A converter macro model);
- there is a strong feedback loop with logic subsystems present;
- the system is too complex to be simulated at transistor level;
- pure behavioral simulation will not give important details such as possible oscillations or glitches.

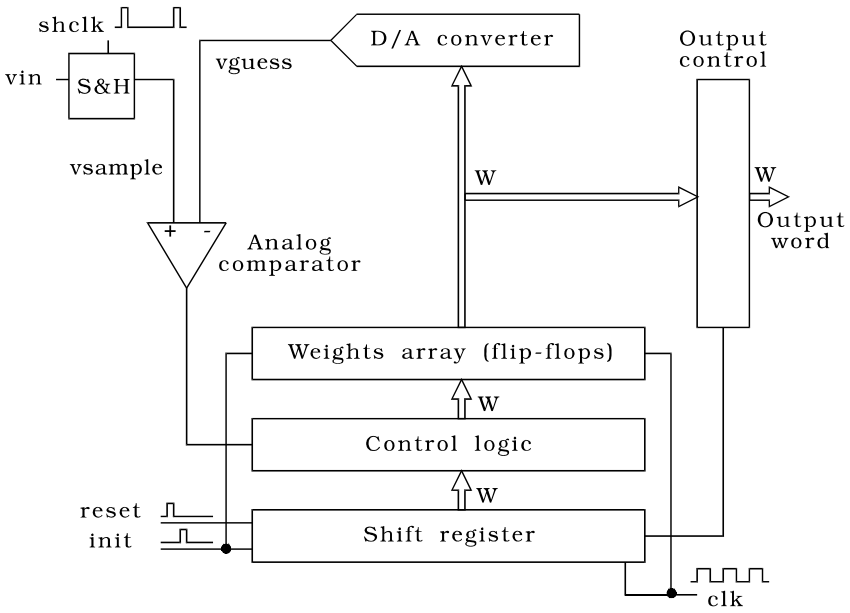

Fig. 5.30: Block diagram of an serial approximative A/D converter

The description of the serial A/D converter started with subsystem interface definition. All of the subsystems modules were parametrized in order to handle different output digital word lengths. In the first refinement, all the

subsystems (analog, digital and hybrid) were implemented as behavioral to obtain crude results. All of the logic modules were modeled at the Register-Transfer Level, i.e. delay times were identical for all the bits in the register data paths. Transfer characteristic of the analog comparator was modeled using general nonlinear generator and *hyperbolic tangens* function, while D/A converter and sample and hold circuit employed dual-process strategy similar to the one used for standard D/A domain-coupling modules implicitly inserted by the simulator. The simulation results of the 8-bit configuration with the slow ramp input are shown in Fig. 5.31.

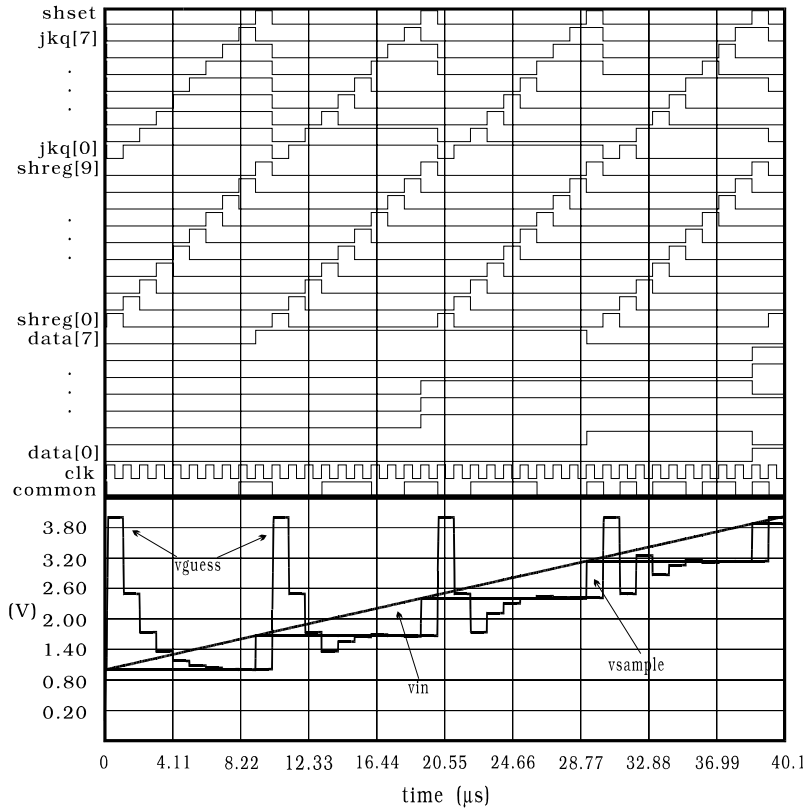

Fig. 5.31: Results of the A/D converter simulation using behavioral representations of the sub-blocks. Digital output variables are at separate plots while analog output variables are all at one plot. Signals data [0] - data[7] represent the output word.

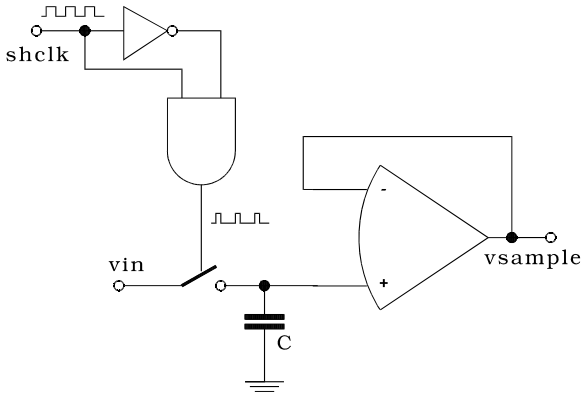

(a)

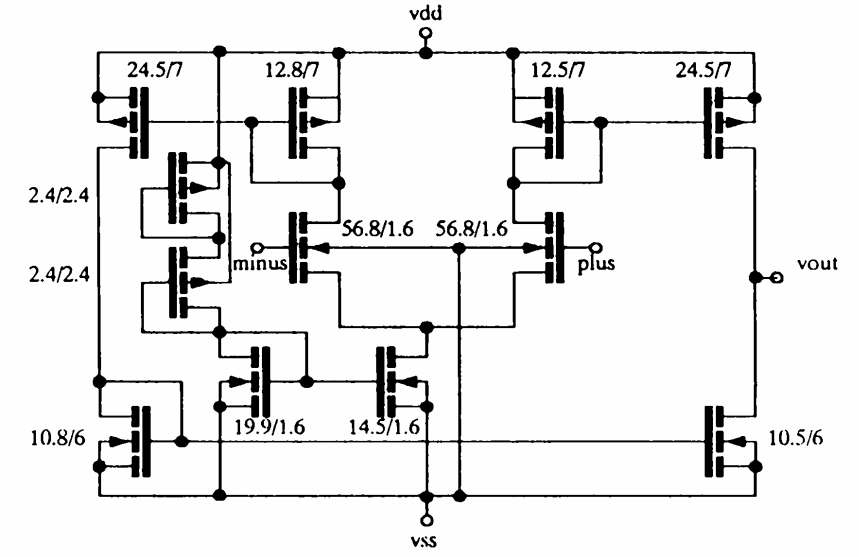

(b)

Fig. 5.32: (a) Structural version of sample and hold sub-block used in the second A/D converter partitioning. The circuit consists of logic gates, internally controlled ideal switch, capacitor and operational amplifier described at transistor level.

(b) Operational amplifier structure. Transistor channel dimensions are given in μm.

The first simulation was very fast due to the high-level behavioral models. In order to obtain a better accuracy, some of the subsystems were further partitioned into smaller blocks. Digital blocks were modeled at the gate-level, using JK and D-type flip-flops and standard logic gates. The sample and hold circuit was replaced with the circuit shown in the Fig. 5.32(a), with ideal switch, capacitor and a CMOS operational amplifier described at transistor level as shown in Fig. 5.32(b). The same amplifier was used as a comparator. This partitioning helped to detect certain instabilities caused by the small phase margin of the operational amplifier. Another problem occurred due to different delay times of the individual JK flip-flops that form the digital output, resulting in noticeable glitches at the D/A converter output. Both effects are shown in the Fig. 5.33. The second simulation was much slower (455 sec with transistor-level CMOS opamps and logic gates as opposed to 4.7 sec in the case of the behavioral model) primarily because of the analog portion of the system.

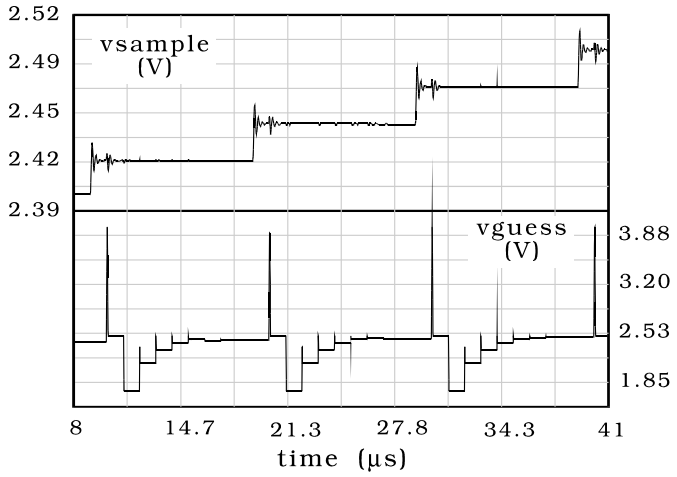

Fig. 5.33: Simulation results of the A/D converter with digital circuits at logic level, and analog at transistor level. Attenuated oscillations at the S&H output and glitches at D/A converter output are now clearly visible.

5.13. Second order sigma-delta modulator

The oversampling sigma-delta conversion technique offers an alternative method of producing high-accuracy, high-resolution ADC's without the need for precise component matching and complex analog circuitry.

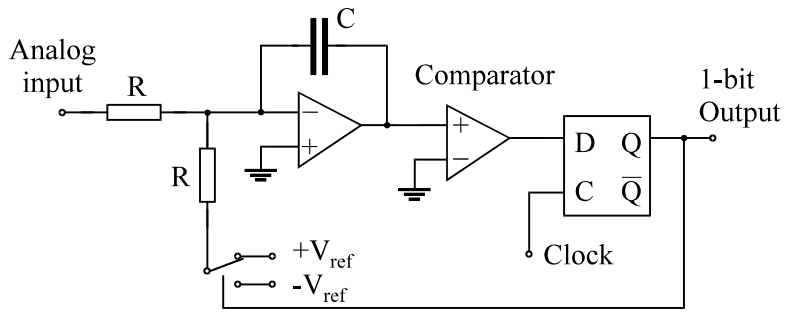

Fig. 5.34: First order sigma-delta modulator.

A first order sigma-delta modulator is shown in Fig. 5.34. The gain of the circuit is given by

$$G = \frac{1}{RC\, f_{clock}}, \tag{5.10}$$

which means that it is dependent on the sampling rate. If the primary gain is designed for the lowest sampling rate, the gain will decrease with increasing sampling rate, reducing the dynamic range of the modulator.

A way to keep the gain constant is to make the integrator charging time invariable with respect to clock rate. This means that the analog switch must be turned on for fixed time duration regardless of clock rate. One solution for achieving this is to use monostable multivibrator as a fixed-width pulse generator in the circuit. A second order sigma-delta modulator with variable sampling rate is shown in Fig. 5.35.

The monostable multivibrator between the clock input and switch control block functions as a pulse generator to produce control signals of fixed time duration. The pulse width is chosen such that the circuit operates at the maximum clock rate of 1.024 MHz. The reference voltages of this circuit are ±1.5 V.

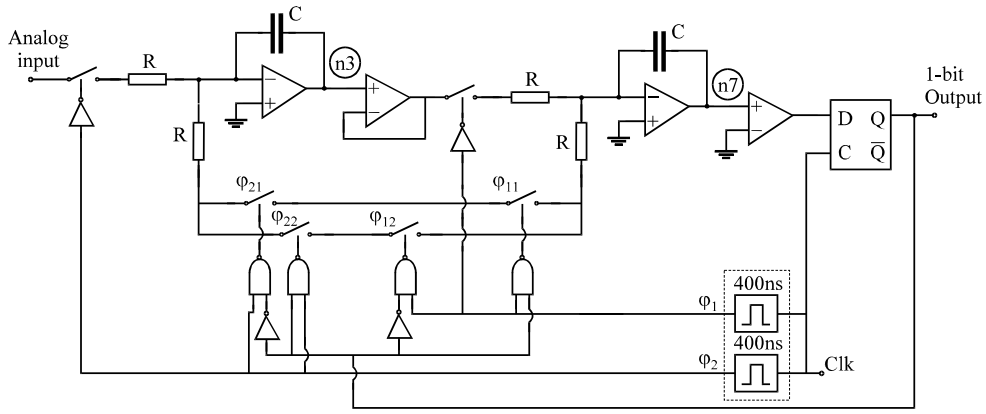

Fig. 5.35: Second order sigma-delta modulator.

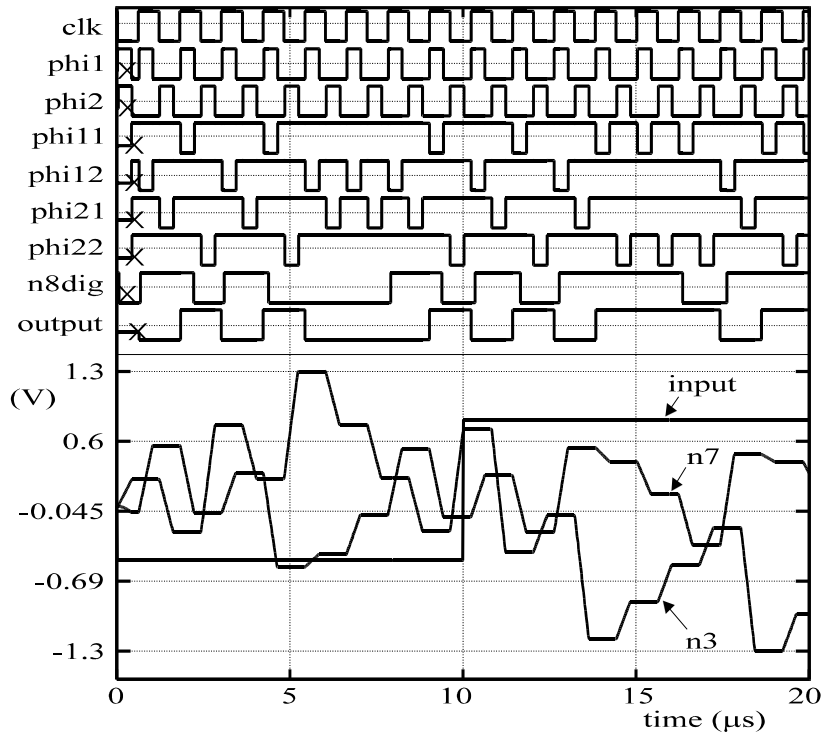

Fig. 5.36: Simulation results of sigma-delta modulator with two-level input excitation.

Results of the simulation, when two levels of a constant analog signal are brought to input, are given in Fig. 5.36. All digital signals in the circuit, and three

analog signals (input, and two voltages at the output of the integrators) are plotted out.

Fig. 5.37 shows reaction of the system when the input is excited by a linear ramp. The simulation time is longer, and the changes of the output can be noticed.

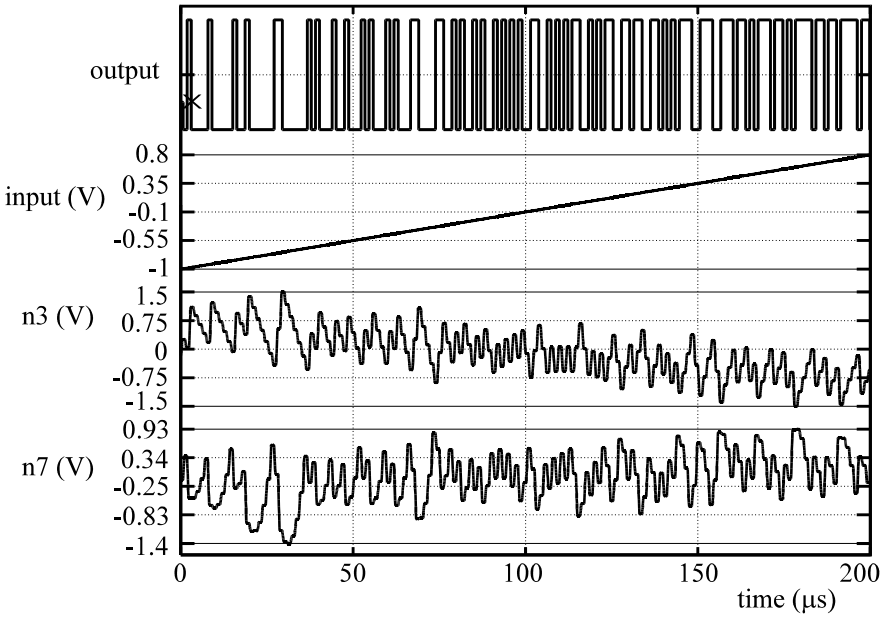

Fig 5.37: Simulation results for linear ramp excitation

5.14. Capacitive pressure sensor followed by A/D conversion

Microsystem development, miniaturization and integration demand more than purely electronic circuit simulator, since mechanical and electrical subsystems are to be fabricated together. Simulation of the complete system is often necessary and cannot be performed with a simulator solely dedicated to electronics or mechanics.

The system considered here is shown in Fig. 5.38.

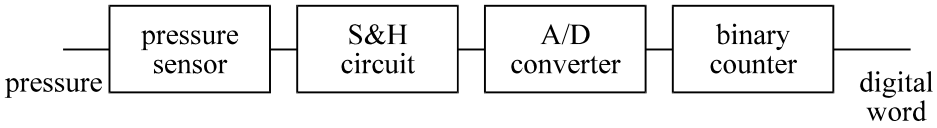

Fig. 5.38: Sensing system

The pressure sensor is a capacitor, where the capacitance is dependent on a plate displacement, and this displacement is a function of pressure. In this example, the plate has circular shape. We presume quasi-static conditions and constant pressure all over the plate. A switched-capacitor pressure sensing system is given in Fig. 5.17. Cs is the sensor capacitance and Cr a reference capacitance.

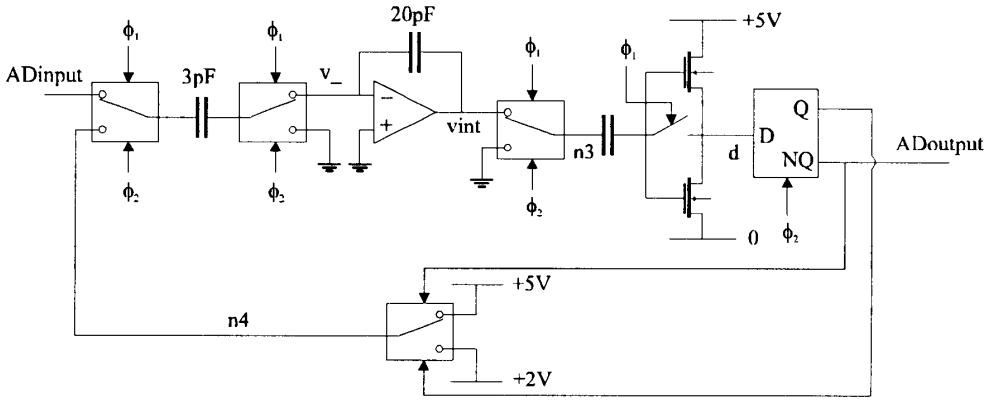

Fig 5.39: Sigma-delta modulator

In real systems there is a need to have digital information about the voltage which refers to input pressure. Since we have discussed quasi-static conditions, the so-called sigma-delta modulator would be a convenient way to perform A/D conversion. Fig. 5.39 shows detailed scheme of a sigma-delta modulator.

When uniform signal is brought to the input, the converter gives the number of pulses proportional to the level of the input signal. The resolution of converted signal is proportional to a time spent in conversion. Logic state of the output signal makes decision whether the signal coming to integrator would be increased or decreased.

The sample and hold circuit as well as the binary counter are described behaviorally. Their structure is not of interest, but their existence is required. All the parts of the system work with a clock signal of 10μs period, and sample and hold circuit has a clock pulse computed from:

$$SHclk = resolution \cdot 10\mu s$$

When resolution parameter is increased, the amount of time needed for gaining one value of pressure is also greater. Since we have discussed quasi-static conditions, this fact is not crucial.

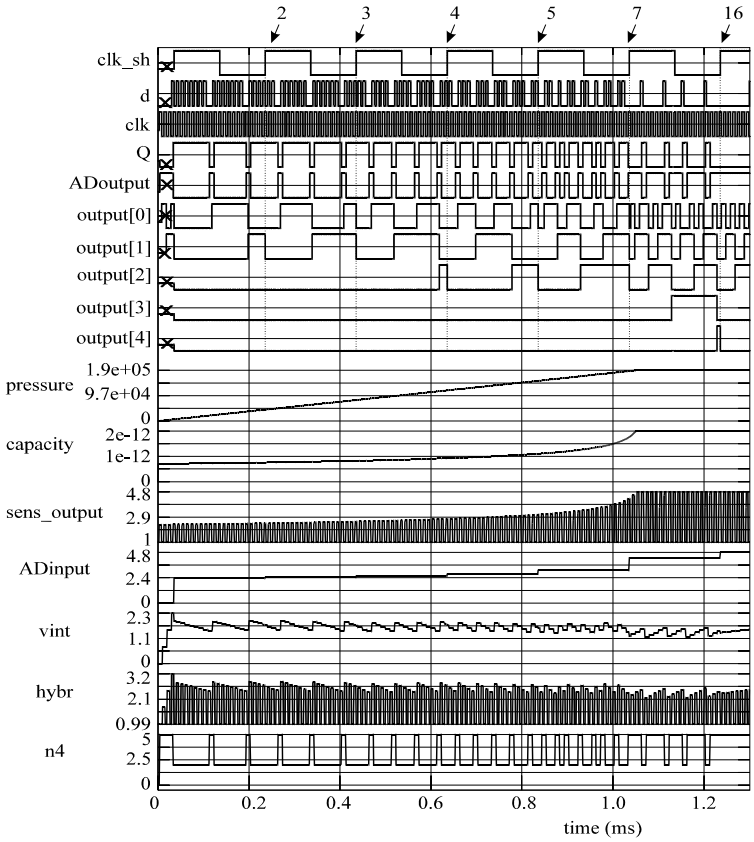

Fig 5.40: Sensing system simulation results

The results of the simulation, when the pressure is monotone and rising, are given in Fig 5.40. The following variables are shown: input pressure signal; capacitance of the nonlinear capacitor; pressure sensor output signal; AD converter input held value; internal converter waveforms - voltage at the integrator output (`vint`), voltage at the input of flip-flop (`hybr`), returned value (`n4`). Digital signals are: `clk_sh` - sample/hold circuit clock signal; `clk` - system clock; `d` - digital value of voltage at node `hybr` obtained at the output of automatically inserted A/D converter interface circuit; `ADoutput` - converter output; `output [0]` to `output[4]` - counter output signals. Counted values are marked below.

Fig. 5.41 shows the system response to sine input pressure, with resolution=100 (`ADinput` is held value and `counted` is counter output). It is easy to observe mapping of sensor nonlinearity to the measured value.

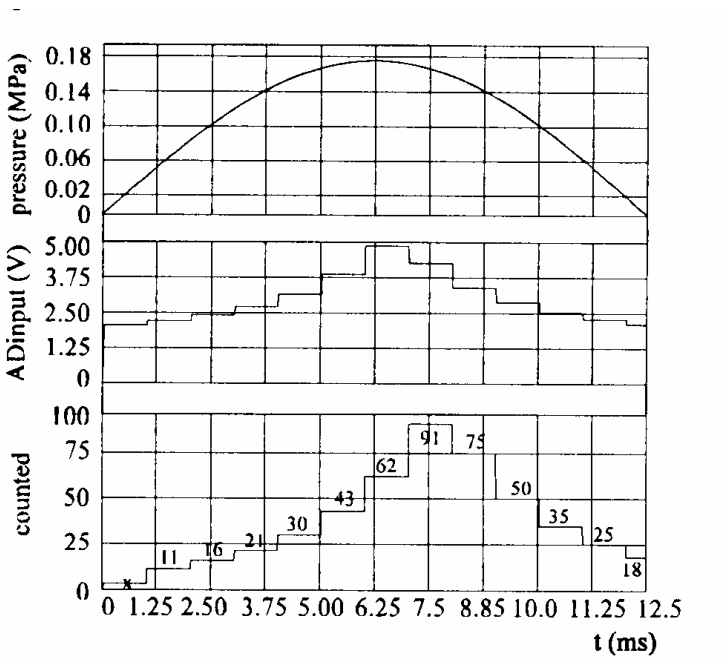

Fig. 5.41: The sensing system response to the sine input signal

5.15. Alecsis-VHDL co-simulation

In this chapter we shall demonstrate the possibility of Alecsis-VHDL co-simulation. To realize this idea we are developing a separate program – VHDL-AMS compiler. The most of VHDL constructs are already implemented, as will be illustrated on a simple example.

There are many digital model libraries developed in VHDL, and there are many experienced VHDL users, too. Therefore, our intention is to enable Alecsis to simulate digital systems described in VHDL. It also assumes simulation of mixed-signal systems keeping the advantage of using VHDL standard libraries for description of digital portion of the system.

The simplest way to achieve Alecsis-VHDL co-simulation was to use the existing simulation kernel of Alecsis simulator (virtual processor), and to develop a new compiler suited for VHDL language. Our VHDL-AMS compiler converts VHDL or VHDL-AMS source code into object code for Alecsis virtual processor. Alecsis object code is designed for mixed-mode simulation. Therefore it supports almost all VHDL and VHDL-AMS modeling mechanisms.

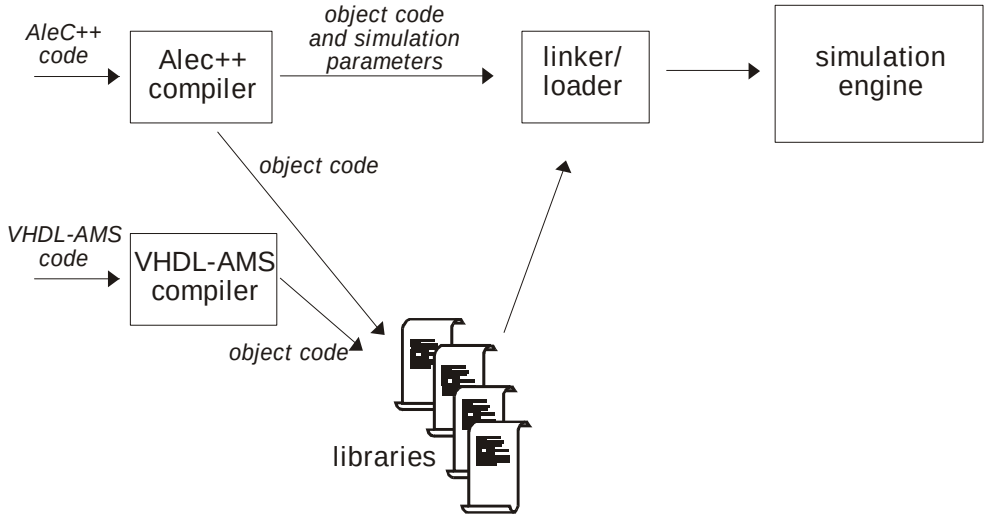

Fig. 5.42: Concept of Alecsis-VHDL-AMS co-simulation

Fig. 5.42 shows the co-simulation concept. VHDL source files are compiled with VHDL compiler and objects are stored into simulation libraries. AleC++ source files are also compiled and objects are stored into libraries of the same format. There is only one important difference. Simulation control parameters cannot be obtained from VHDL code. In other words, the root module must be described in AleC++. The simulation engine cannot make difference between library objects obtained from VHDL and AleC++ compiler.

The basic structural unit in VHDL - entity is converted into AleC++ structural unit - module. Each architecture of an entity becomes a new module with the name equal to the name of the architecture. Generic parameters correspond to module action parameters. The data types in VHDL and AleC++ have different names, but the correspondence can easily be established due to the same machine representation. Type *real* from VHDL corresponds to type *double* in AleC++, *integer* to *int*, *records* are related to *structures*, etc. Structural hierarchy is fully supported both in AleC++ and VHDL. It is possible in VHDL description to instantiate components and to call functions described in AleC++ and vice versa. References to those components and functions will be resolved by the linker/loader before the start of the simulation.

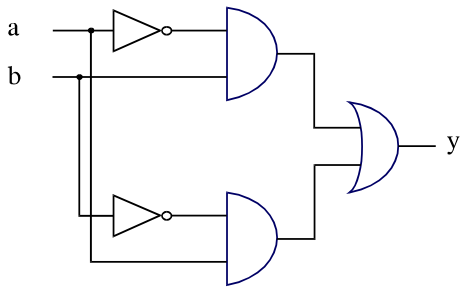

Fig. 5.43: An exclusive-OR circuit

For the illustration of Alecsis-VHDL co-simulation, we shall model a simple circuit shown in Fig. 5.43 with combination of AleC++ and VHDL code. The modeling technique will not be the optimal one, but is intended to be a good illustration of co-simulation possibilities. Fig. 5.44 explains model hierarchy. Inverter (module `inv`) is modeled in AleC++. AND circuit as well as OR circuit is modeled in VHDL (architectures `and2` and `or2`). Inverter and AND circuit are then combined into the AleC++ module named `inv_and`. The whole circuit shown in Fig. 5.43 is described in VHDL and named `xor2`. The delay `delay_f` function used both in AleC++ and VHDL is defined in VHDL.

The simulation is performed in 2-state logic system (signals are of `bit` type). The AleC++ description of module `inv` follows:

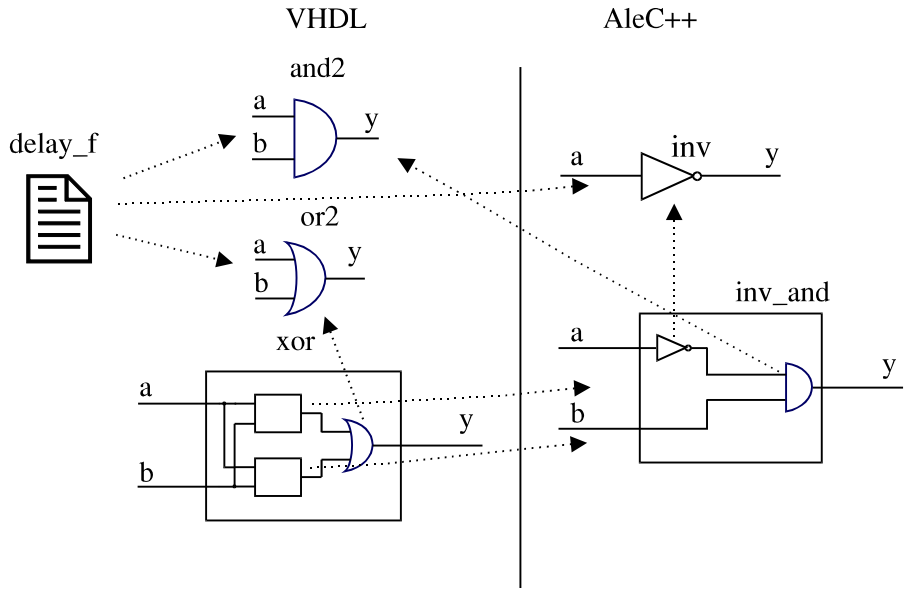

Fig. 5.44: Model hierarchy for circuit from Fig. 5.43

```
double delay_f (bit, double, double); // func. declaration

typedef enum { '0', '1' } bit;  // state system definition

bit const not_tab[] = { '1','0' };

bit operator ~ (bit op) { return not_tab[op]; }

module inv (bit out y; bit in a) {
  action (double tr, double tf){
    process (a) {
      y <- ~a after delay_f (~a, tr, tf) ;
    }
  }
}
```

The function `delay_f` is defined in VHDL. AleC++ only requires its declaration to be visible before the function call, because of type-checking mechanism. Function code is rather trivial.

```
--- Standard gate delay function:
function delay_f (state: bit; tr: real; tf: real)
                                        return real is
begin
  if state='0' then
    return tf;  --fall time
  else
    return tr;  --rise time
  end if;
end delay_f;
```

OR and AND circuits are modeled with the next VHDL code.

```
--- Two-input AND gate:
entity and2_e is
  generic (tr: real := 1.0e-9; tf: real := 1.0e-9);
  port (y: out bit; a,b: in bit);
end and2;

architecture and2 of and2_e is
begin
  process(a,b)
  begin
    y <= a and b after delay_f(a and b, tr, tf);
  end process;
end inv;

--- Two-input OR gate:
entity or2_e is
  generic (tr: real := 1.0e-9; tf: real := 1.0e-9);
  port (y: out bit; a: in bit; b: in bit);
end or2_e;

architecture or2 of or2_e is
begin
  process(a,b)
  begin
    y <= a or b after delay_f(a or b, tr, tf);
  end process;
end or2;
```

The block composed of an inverter and an AND circuit (`inv_and`) is described in AleC++ code that instantiates VHDL component `and2`. Structural modeling is used.

```
module inv_and ( bit out y; bit in a; bit in b) {
  signal bit inter; // internal signal, inverter output
  module inv inverter;     // modeled in AleC++
  module and2 and_circ;    // modeled in VHDL

  inverter (inter,a)   { tr=1ns;tf=0.9ns; }
  and_circ (y,inter,b) { tr=1ns;tf=0.9ns; }
}
```

The whole circuit is modeled in VHDL and named `xor2`. It is composed of two components `inv_and` and the component `or2`.

```
--- Two-input XOR gate:
entity xor2_e is
  port (y: out bit; a: in bit; b: in bit);
end or2_e;

architecture xor2 of xor2_e is
  component or2
    generic (tr: real; tf: real);
    port (y: out bit; a, b: in bit);
  end component;
  component inv_and
    port (y: out bit; a: in bit; b: in bit);
  end component;
  signal inter1,inter2: bit;           -- internal nodes
begin
  -- modeled in AleC++
  c1: inv_and port map (inter1,a,b);
  c2: inv_and port map (inter2,b,a);
   -- modeled in VHDL
  c3: or2 generic map (tr=>1.0e-9, tf=>0.8e-9)
          port map (y,inter1,inter2);
end xor2;
```

Finally, to simulate exclusive-OR circuit, it is necessary to have a root module in order to define circuit stimulus and simulation control parameters. The following code represents a simple root module for testing the module `xor2` by checking its output state for all input vectors.

```
library "xor";
root module xor_circuit_test (){
  signal bit a, b, y;
  module xor2 g1;


  g1 (y, a, b);
```

```
    out { signal bit a, b; signal bit y; }

    timing { tstop = 30ns; }
    action {
      process initial {
          a <- '1' after  5ns, '0' after 15ns;
          b <- '1' after 10ns, '0' after 20ns;
      }
    }
  }
```

Simulation results are shown in Fig. 5.45.

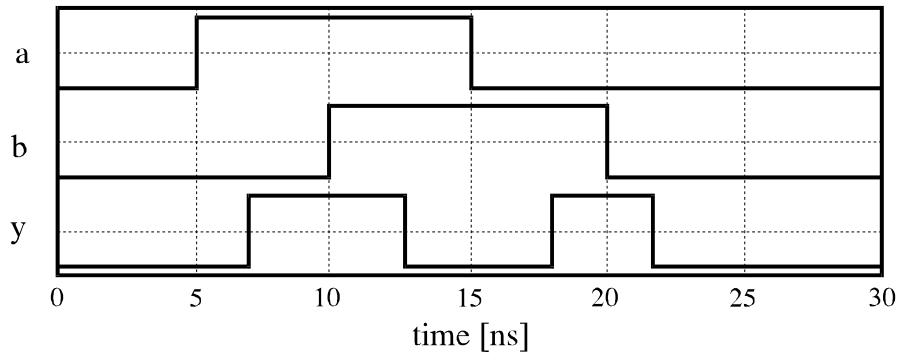

Fig. 5.45: Simulation results for exclusive-OR circuit shown in Fig. 5.43.

5.16 AleC++ - VHDL-AMS co-simulation

VHDL-AMS modeling environment in Alecsis is also supported by the compiler described in the previous section.. The co-simulation concept is the same as it is shown in Fig. 5.42.

Since AleC++ resembles the semantics of standard HDLs, such as VHDL-AMS, the correspondence between language elements can be easily established (Fig. 5.46).

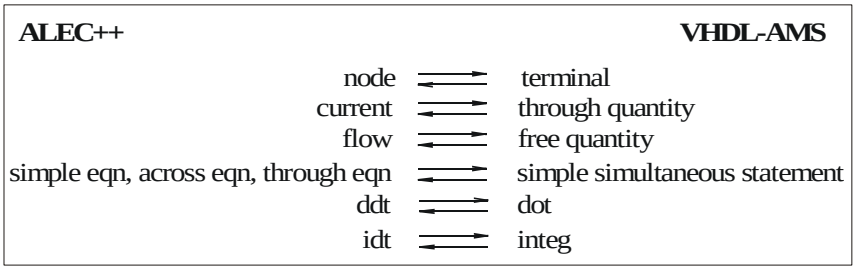

Fig. 5.46. Correspondence between AleC++ and VHDL-AMS

For describing of continuous systems VHDL-AMS uses the theory of differential and algebraic equations (DAE's). A new class of objects, the *quantity*, is introduced to represent the unknowns in the system of DAE's. Also, special kind of quantities called *branch quantities* are used for representing the unknowns in the equations describing conservative systems (systems obeying Kirchhoff's laws). There are two types of branch quantities: *across quantities* (for effort like effects such as voltage or pressure) and *through quantities* (for flow like effects such as current or fluid flow rate). They are declared with reference to two terminals representing nodes of the module. AleC++ uses a similar language element called *link* to describe quantities that appears on a module terminal and represent the unknowns in the behavioral system descriptions. There are five types of links in AleC++: *node*, *current*, *flow*, *charge*, and *signal*. Obviously, node corresponds to a terminal and current to a through quantity. The flows represent general analog quantities and correspond to free quantities in VHDL-AMS. Simple simultaneous statements used for notating DAE's in VHDL-AMS relate to appropriate AleC++ constructs for writing equations. Since the way of writing equations is almost the same in both languages VHDL-AMS compiler can easily determine contributions of the equations from VHDL-AMS model to the matrix of the system of equations describing the whole design. It is necessary in Alecsis to explicitly specify to which matrix row the equation contributes. In equations using free quantities that information can be provided as the equation's label. In equations containing branch

quantities terminals can be used to determine matrix rows to which equations contribute.

VHDL-AMS provides conditional and selected forms of the simultaneous statement that allow changing set of equations in the model. Since AleC++ has similar constructs, VHDL-AMS compiler can easily translate those statements into the corresponding object code.

Both languages support signal attributes for derivative and integration over time used in differential equations. AleC++ also supports second-order time derivative attribute and it is implemented in VHDL-AMS compiler, too.

In order to illustrate AleC++/VHDL-AMS mixed-language description and simulation we shall model a mechanical system describing oscillating mass. The structure of the model is shown in Fig. 5.47.

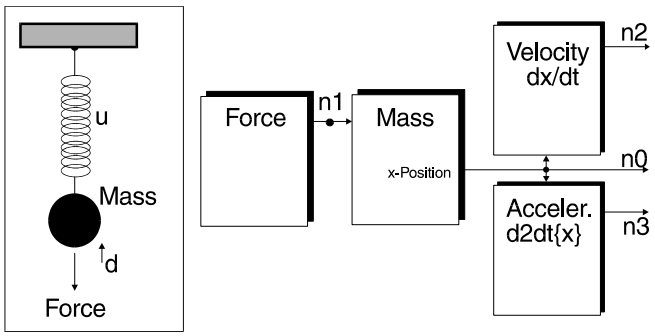

Fig. 5.47. The structure of oscillating mass model

The architecture of the mass is described in VHDL-AMS and defines mechanical equilibrium as a single second-order differential equation using a simple simultaneous statement:

```
entity mass_e is
       generic (m,u,d: real);
       port (quantity x: out real;
             quantity force: in real
);
end entity mass_e;
architecture mass of mass_e is
begin
     x:  m*x'dot'dot + d*x'dot + u*x - 1*force == 0;
end architecture mass;
```

Entities for calculating velocity and acceleration are not necessary for simulation, but are used just to print out the appropriate results:

```
entity velocity_e is
       port (quantity x: real;
             quantity v: real
);
end entity velocity_e;

architecture velocity of velocity_e is
begin
       v:  1*v - 1*x'dot == 0;
end architecture velocity;
```

```
entity acceleration_e is
       port (quantity x: real;
             quantity a: real
);
end entity acceleration_e;

architecture acceleration of acceleration_e is
begin
       a:  1*a - 1*x'dot'dot == 0;
end architecture acceleration;
```

The model stimulus is described in AleC++:

```
module Force (flow force) {
       action (double force_value) {
              double force_out;
              process per_moment {
                     force_out = force_value*exp(-now);
                     eqn force: {force} = force_out;
              }
       }
}
```

In order to simulate the system all models are instantiated and appropriate simulation control parameters are defined in a root module described in AleC++:

```
      #include <alec.h>
      #define Period 15. s
      module mass_mod(flow x, force) action(double m, double u,
double d);
      module velocity_mod(flow x, v);
      module acceleration_mod(flow x, a);

      library "mass";
      library "velocity";
      library "acceleration";

      module Force (flow force) {
            action (double force_value) {
                  d ouble force_out;
                  process per_moment {
                        force_out = force_value*exp(-now);
                        eqn force: {force} = force_out;
                  }
            }
      }

      root eq() {
            flow n0, position, velocity, acceleration;
            mass_mod p;
            Force F;
            velocity_mod V;
            acceleration_mod A;

            p(position,n0) {m=1; u=1; d=0.35;}
            F(n0) {force_value=10;}
            V(position,velocity);
            A(position,acceleration);

            timing {tstop = Period; a_step = Period/1000;}
            plot {flow position;flow velocity;flow acceleration;}
}
```

VHDL-AMS models have to be compiled first into the AleC++ object code by using VHDL-AMS compiler. Then, the whole system is simulated using Alecsis.

The mixed-language simulation results are shown in Fig. 5.48. Traced signals are positon, velocity and acceleration, respectively.

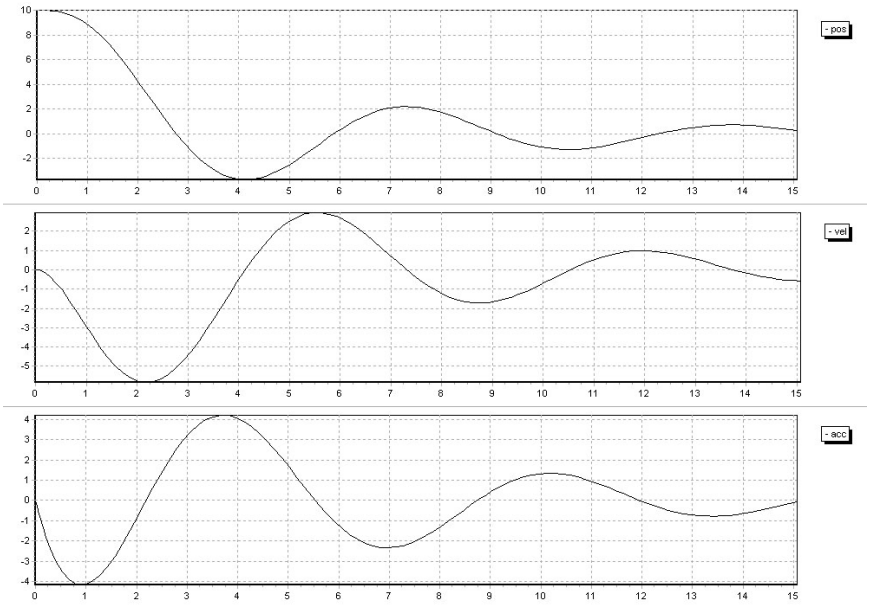

Fig. 5.48. Simulation results of the oscillating mass shown in Fig. 5.47.

5.17. Bouncing ball -- discontinuity example

Most of classical simulators cannot cope with the discontinuity of the system's behavior when it occurs during the simulation. This means that systems that have response that is not differentiable cannot be simulated with such simulators. Primary reason is the way in which a simulator works: for finding the solution in one time point it needs solution(s) in one (or more) past point(s), depending on the integration method.

Excellent, while simple example of discontinuity is bouncing ball. Discontinuity occurs when the ball reaches ground. The sign of velocity is changed and the ball rebounds. It is of crucial importance to extract the "discontinuity" instant, so that the simulator can react by calculating new initial conditions.

The idealized ball's trajectory is described by the equation:

$$\frac{d^2x}{dt^2} + g + \rho \cdot \left(\frac{dx}{dt}\right)^2 = 0 \qquad (5.11)$$

where g is the gravity constant and ρ the air damping coefficient.

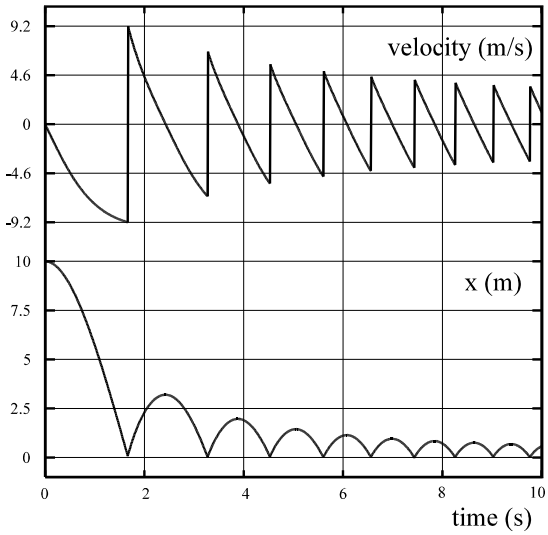

Fig. 5.49: Simulation results for bouncing ball

Discontinuity is determined when x falls down to zero. The results of the simulation are given in Fig 5.49. Lost of energy due to the impact is not considered in this example.

5.18 Modeling of D/A interface for mixed-mode behavioral simulation

The design of electronic and telecommunication integrated circuits is unavoidably faced with simulation of analogue subsystems of ever rising complexity thereby building more complex mixed-signal systems containing both analogue and digital parts. Design of such systems needs simulation tools that perform fast and accurate in the same time. Main obstacle to this requirement is related to the difficulties in high level modeling of the analogue part and accurately enough modeling of the digital-analogue (D/A) and analogue-digital (A/D) interfaces being frequently encountered in such systems. In fact at the (D/A) interface one needs to model the output circuit of the digital part in order to enable electrical excitation for the analogue load. In the opposite case, at the (A/D) interface, we need to model the input impedance of the digital part in order to establish conditions for computation of the voltage and current at the interface. Having in mind that the simulation is performed in the time domain, the fact that we are dealing with mixed-level simulation, and the complexity and non-linearity of the circuits involved, one generally applies behavioral modeling for these purposes.

We will consider here the situation when the signal is transmitted from the logic to the analogue element, and then we need digital to analogue conversion. Since the load is analogue, there is a problem in generating of the signal waveform on the output of the digital circuit. Modeling of D/A node is very complex because one needs to get the waveform of the signal that drives the analogue part of the circuit out of the set of logic states. The conversion algorithms are mostly based on the synthesis of the electronic circuit that replaces the logic element, and that is applied as excitation to the actual node. The propagations of the logic elements should also be considered.

The following solution is based on artificial neural networks. It is considered very convenient because the function is approximated using the measured values, and no electronic circuit synthesis is needed.

A new topology of the circuit is proposed for this purpose, being depicted in Fig. 5.50.

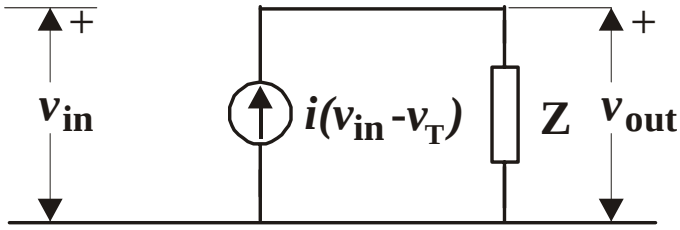

Fig. 5.50. Circuit representation of the model

An inverter is considered here, and v_{in} stands for a controlling ramp-shaped voltage-waveform,

$$i(v_{in} - v_T) = I_{max}\left[1 - \text{th}(v_{in} - v_T)\right], \tag{5.12}$$

and Z is a time delay recurrent neural network approximating the function

$$v_{out} = Z(i) \tag{5.13}$$

I_{max} is the maximal supply current during the transition in the inverter, and v_T is (usually) equal $V_{DD}/2$, V_{DD} being the supply voltage. Obviously, the ANN model of Z has one input (current) and one output (voltage) terminal. The training of the network is performed based on training pairs (i(t), v_{out}(t)), where i(t) is calculated from (5.12) while v_{out}(t) is obtained from simulation of the circuit to be modeled (here inverter). The neural network is a time delay recurrent network (Z), with one hidden layer, five input, three hidden and one output neuron.

Inverter has only one input, so the value of v_{in} voltage is only one. When we are dealing with multi-input circuits, there exist more input voltages because for every combination of inputs there is corresponding output impedance. Also, there is a problem with sequential circuits because the output state depends on input states, as well as on previous output state. During the logic simulation, there always exists information about the events and time of their happening, so it is known what inputs caused certain state and which impedance should be applied to the certain node.

The first results are shown in Fig. 5.51. Here output waveforms of the original inverter and the model are shown in order to show the quality of the approximation procedure. Unloaded circuits are simulated. A behavioral simulator, Alecsis is used to exercise such model.

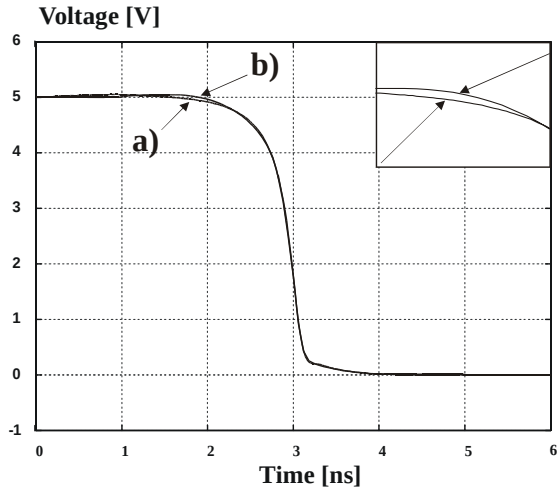

Fig. 5.51. Digital-analogue interface modeling a) response of an unloaded CMOS inverter (considered as digital output) and b) of the new model

The following three examples are intended to check the modeling procedure based on situations not present during the training procedure. Fig. 5.52 represents two responses. The first trace is the output voltage of an inverter (all modeled by regular transistor models) being loaded by inverter. The second one represents the response of the same circuit with ANN model used for the driving part and circuit model for the loading. This situation was unknown in the modeling process.

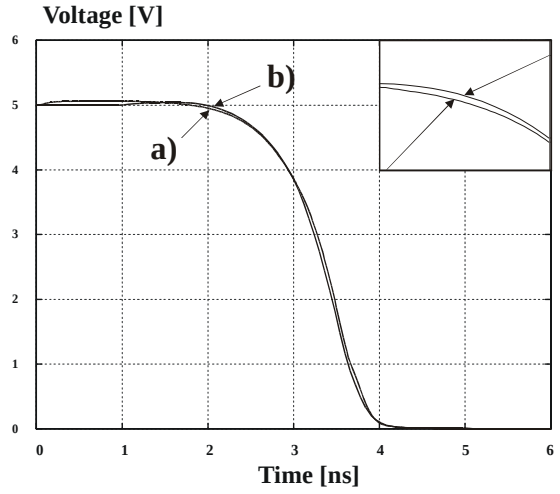

Fig. 5.52. Digital-analogue interface modeling. a) response of an inverter loaded by inverter and b) of a model loaded by inverter

Further, Fig. 5.53 represents similar comparison the loading element being a transmission line modeled by a π -*RC* network.

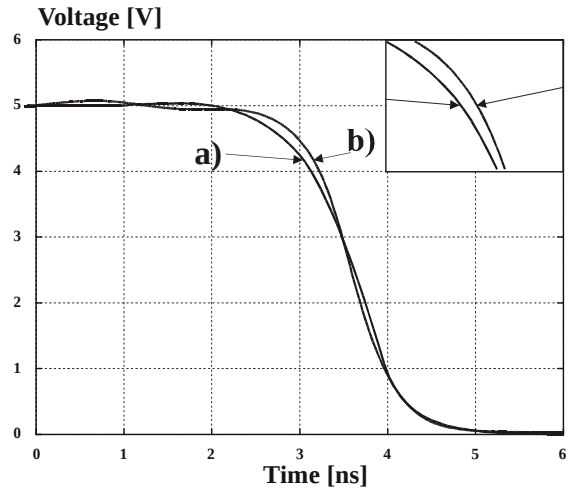

Fig. 5.53. Digital-analogue interface modeling. a) response of an inverter loaded by RC π -network and b) of a model loaded by RC π -network

Finally, a diode load was used to demonstrate the successfulness of the ANN model in the case of "large" non-linear dynamic load. The comparison of the circuit simulation and behavioral simulation are given in Fig. 5.54.

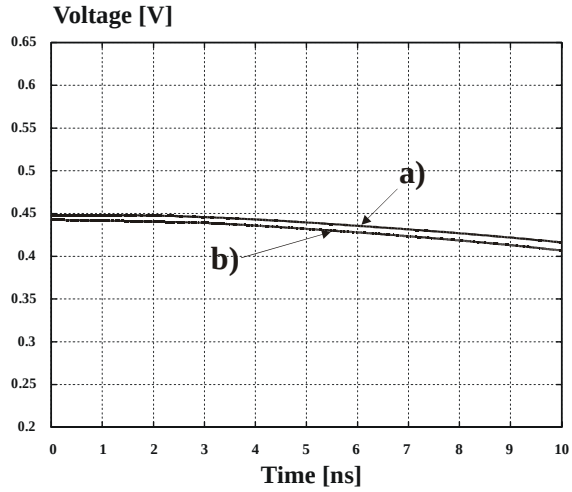

Fig. 5.54. Digital-analogue interface modeling. a) response of an inverter loaded by diode and b) of a model loaded by diode

5.19 Frequency domain simulation

In addition to time-domain simulation, Alecsis simulator also enables the frequency domain simulation. Following examples illustrate this feature.

In order to implement AC domain simulation input language of Alecsis simulator had to be extended. First a new command `ac` for AC analysis has been added. E.g.

```
ac {fscale=2;fstart=10;fstop=1G;fnum=100;}
```

The AC analysis works with complex numbers, and since AleC++ is an object oriented language, all the variables have been added following properties: `amp` (amplitude), `phase` (phase), `real` (real part) and `imag` (imaginary part). E.g. `output->phase` gives the phase of the output. Also a `dc_value` property is added providing the value of the variable after dc simulation, which can be very useful during small-signal modeling.

New types of independent generators have been added as well. Those are `vac` - voltage and `cac` - current generator. They accept following parameters: `amp` - amplitude and `phase` - phase of the signal.

The lists of parameters for any type of controlled sources have been extended. For example, voltage controlled voltage source, beside the `gain`, that now becomes real part, `igain` parameter has been added, representing the imaginary part of complex gain.

New type of process with `per_frequency` synchronization has been supplied, providing the user to write AleC++ code to be processed per frequency. Operator `currfreq` is introduced, returning the current frequency of the simulation. Operator `domain` returns the current simulation domain.

In order to enable the behavioral simulation in frequency domain, equations with complex matrix entries are implemented. There are three types of equations: *simple*, *through* and *across*.

Behavioral description of a capacitor using through `eqn` statement is:

```
module my_capacitor (node i, j){
  action (double value=1.e-15){
...
    process per_frequency {
      double y = 2*M_PI*value*currfreq;
      eqn {i, j}.i = y*{i->im, j->im}.v;
    }
  }
}
```

All these features, along with object-orientedness of the AleC++ provide a powerful tool for behavioral frequency domain simulation.

As a simulation example for passive circuits, a ten stage crystal band-pass filter shown in figure 5.55.a has been simulated. Obtained amplitude characteristic is shown in figure 5.55.b.

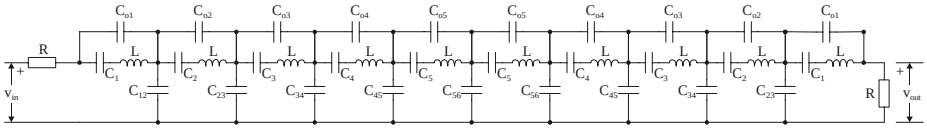

Fig. 5.55.a: Ten-stage crystal band-pass filter

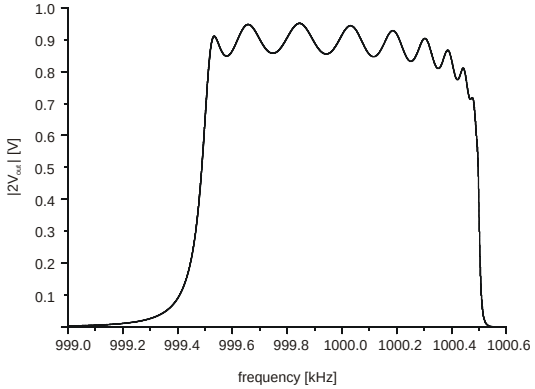

Fig. 5.55.b: Amplitude characteristic

As an example for simulation of active circuits, two-stage frequency compensated MOS amplifier, shown in Fig. 5.56, was simulated. Transistor M_{13} has a function of a zero-canceling resistor. Transistors M_{14}, M_{15} i M_{16} bias this transistor.

Fig. 5.57 gives the simulation results for variation of channel width of the M_{15} transistor.

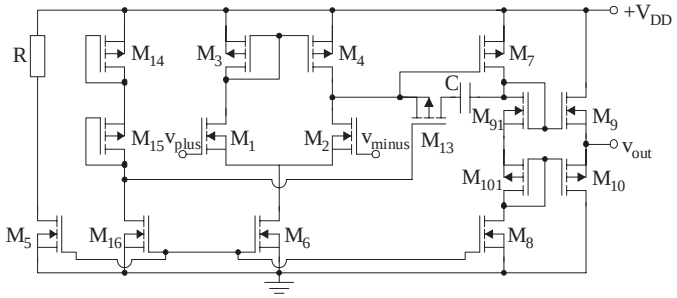

Fig. 5.56: Two-stage operational amplifier

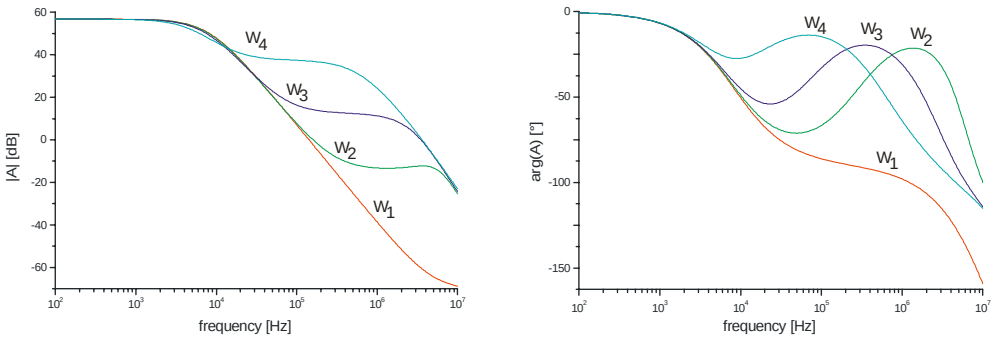

Fig. 5.57: Amplitude and phase for the variation of channel width of M_{15}

The following example illustrates the fully behavioral description using controlled sources. Fig. 5.58 shows the simulated circuit. Block named *core* can model virtually any circuit. All the parameters of the block (here h - parameters) can be assigned functions of arbitrary complexity. Combination of circuit and behavioral model is used. Sample of simulation code in AleC++ shows how one of the core parameters is calculated. The results of the simulation are depicted in Fig 5.59. Complex class enables complex arithmetics.

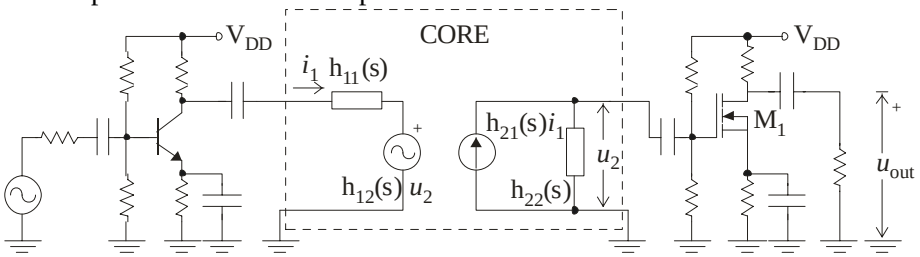

Fig. 5.58: Simulated circuit

```
#include <complex.ac> //complex class
...
root module test_circuit()
{
  IP_core ip;
...
  ip (3, 0, 4, 0);
...
  action per_frequency (){
    double h210 = 100 + 1.5*(VDD - 6);
    double w = currfreq/(2*M_PI);
    double wz1 = 10/(2*M_PI);
    complex s(0, w);
    complex h21 = h210*(s/wz1+1);
...
    ip->h21r = h21.real;
    ip->h21i = h21.imag;
...
  }
  ac{fscale=2; fstart=1; fstop=10MEG; fnum=10;}
}
```

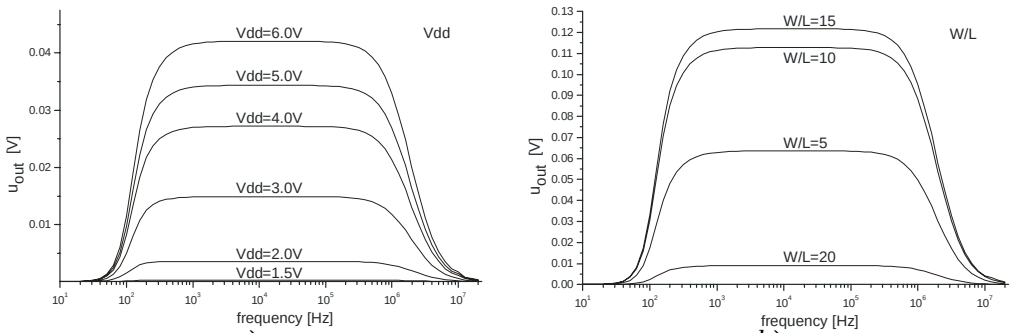

a) *b)*

Fig. 5.59: Simulated results: output voltage for variations of a) Vdd and b) W/L ratio of the M1 transistor

Another example represents the behavioral modelling of the BJT. Sample of the AleC++ code shows how capacitors are modeled behaviorally using eqn statements.

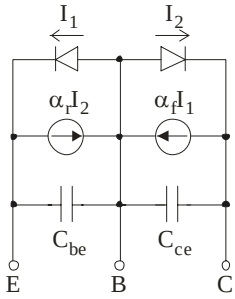

Fig. 5.60: Ebers-Moll model of the BJT

```
#include <alec.h> //standard header
...
     process per_frequency {
      double Vbe_dc, Vbc_dc, alpha, gdbe, gdbc, cbe, cbc;
      alpha = 1/vt;
      Vbe_dc = (node) b->dc_value - (node) e->dc_value;
      Vbc_dc = (node) b->dc_value - (node) c->dc_value;
      gdbe = i0/vt*exp(alpha*Vbe_dc);
      gdbc = i0/vt*exp(alpha*Vbc_dc);
      cbe = tau*gdbe //diffusion component
           + Cbe_junc*pow((1-Vbe_dc/vt), -0.5);
                     //junction component
      cbc = tau*gdbc //diffusion component
           + Cbc_junc*pow((1-Vbc_dc/vt), -0.5);
                     //junction component
      eqn {b, e}.i = gdbe*{b, e} - ar*gdbc*{b, c} +
                     2*M_PI*cbe*currfreq*{b->im, e->im}.v;
      eqn {b, c}.i = gdbc*{b, c} - ar*gdbe*{b, e} +
                     2*M_PI*cbc*currfreq*{b->im, c->im}.v;
    }
...
```

5.20 Space-continuous analogue systems

Circuit simulation normally uses so-called lumped models – continuous in time, but discrete in space. However, deep submicron designs and mixed-domain systems (semiconductor sensors and actuators) often demand introduction of models that cannot be correctly defined with lumped models.

A solution can be to define space-continuous models as a set of lumped models. In standard circuit simulators, this can lead to extremely large input files, which also makes design errors intraceable. However, AleC++ posses a mechanism to define arrays of lumped analogue models using simple syntax costructions. For instance, array of finite elements that describe thermal or mechanical behavior can be contained in a module named **elementary_matrix**. An array of such matrices can be defined in **process structural**:

```
module finite_element model( … ) {

   /* declaration */
   module el_matrix EM;
   node n1[auto]; // declaration of nodes
   node n2[auto]; // that will be dynamically
   ….             // allocated

   /* structure is here omitted, as it
      will be given in process structural */
   action(double size_n1,
          double size_n2,
          double no_of_elems) {
      process structural {
         allocate n1[size_n1];
         allocate n2[size_n2];
         int i;
         for (i=0; i<no_of_elems; i++) {
            clone EM[i] (n1[i-1],n2[i-1],...);
         }

         …
      }
   }
}
```

This feature had been extensively used in Alecsis for transmission line modeling, micromechanical systems simulation, thermoelectrical simulation, and smart-material analysis.

In Fig. 5.57, finite element simulation results obtained using ANSYS simulator for temperature distribution on a chip are shown. Fig. 5.58. shows the same results obtained using Alecsis. The relative error is smaller than 0.005% for static analyses. Comparable results may be achieved in transient simulation with coupled electronic components.

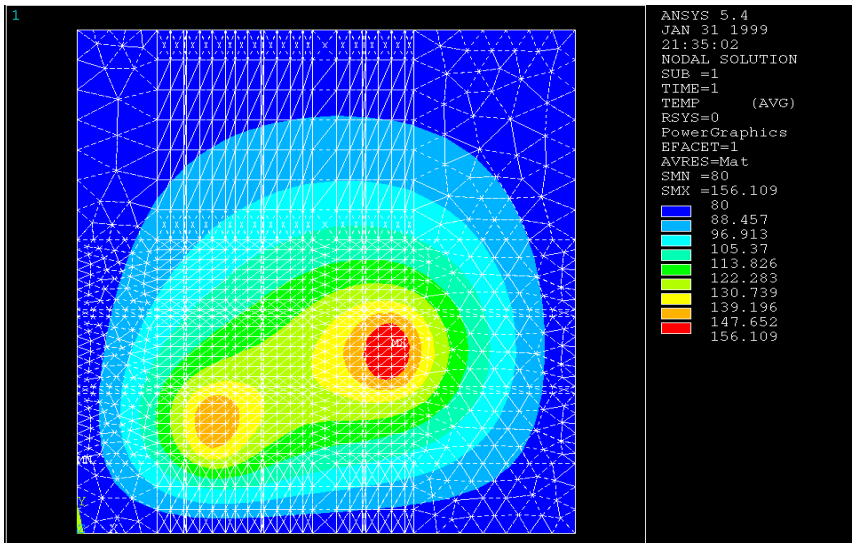

Fig. 5.57. Temperature distribution on the chip (ANSYS results)

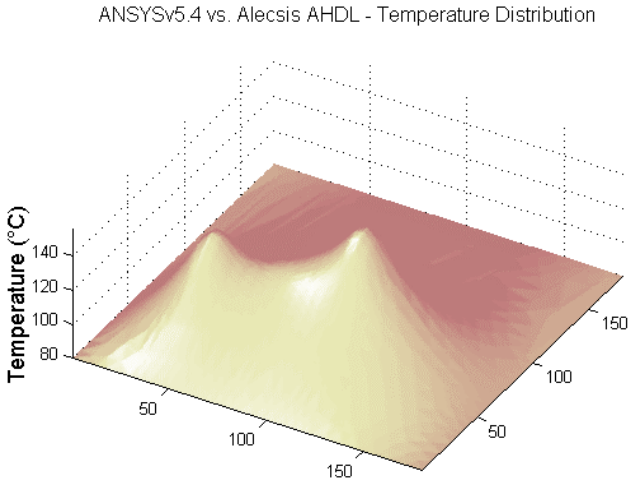

Fig. 5.58. Temperature distribution on the chip (Alecsis simulation/MathCAD visualizatison)

The application of mixed-domain simulator with analog hardware description languages and mixed analog/digital simulation seems to be promising for this class of engineering problems.